Spatio-Temporal analysis of drought and return periods over the East African region using Standardized Precipitation Index from 1920 to 2016

Wilson Kalisa[1,2], Jiahua Zhang[2,3*], Tertsea Igbawua[4], Fanan Ujoh[5], Obas John Ebohon[5], Jean Nepomuscene Namugize[6], Fengmei Yao[7]

1. Agricultural Climate Change Mitigation, College of Automation and Electrical Engineering, Qingdao University, Qingdao, 266071, China

2. Remote Sensing and Digital Earth Center, College of Computer Science and Technology, Qingdao University, Qingdao, 266071, China

3. Key Laboratory of Digital Earth Science, Aerospace Information Research Institute, Chinese Academy of Sciences, Beijing, 100094, China

4. Department of Physics, Federal University of Agriculture, Makurdi, Nigeria

5. Center for Sustainability and Resilient Infrastructure and Communities (SaRIC), School of the Built Environment and Architecture, London South Bank University, London, UK

6. Rwanda Polytechnic, Integrated Polytechnic Regional Center, College of Kigali, Rwanda

7. Key Laboratory of Computational Geodynamics, University of Chinese Academy of Sciences, Beijing, 100049, China

*Corresponding- author: Prof. Jiahua Zhang, email address: zhangjh@radi.ac.cn

Revised to "*Agriculture Water Management*"

Abstract East African region is susceptible to drought due to high variation in monthly precipitation. Studying drought at regional scale is vital since droughts are considered a 'creeping' disaster by nature with devasting and extended impact often requiring long periods to reverse the recorded damages. This study assessed drought exceedance and return years over East Africa from 1920 to 2016 using Climate Research Unit (CRU) precipitation data records. Meteorological drought, where precipitation is the central quantity of interest, was adopted in the work. Standardize Precipitation Index (SPI) was used to study long term meteorological droughts and also to assess drought magnitude, frequency, exceedance probability and return years using Joint Probability Density Function (JPDF). Also, Mann-Kendall trend analysis was applied to precipitation and SPI to investigate the trend changes. Results showed that years with high drought magnitude ranged from 1920-22, 1926-29, 1942-46 and 1947-51 with values corresponding to 2.2, 3.2, 3.4 and 2.6, respectively while years with low drought magnitude ranged from 1930-31, 1988 89 and 2001-02 with values as 0.2, 0.12 and 0.15, respectively. The longest droughts occurred from 1926-29, 1937-41, 1942-46, 1947-51, 1952-56, and 1958-61 with values in years as 3, 4, 4,

4, 4, and 3 years, respectively, while the shortest droughts occurred in time period of 1 year and ranged from 1930-31, 1964-65, 1979-80, 1981-82, 1983-84, 1988-89, 1991-92, 1993-94, 1996-97 and 2001-02. Also, it was demonstrated that probability of drought occurrence is high when severity is low and such droughts occur at short time intervals and not all severest drought took longer periods. The SPI trends indicate high positive (negative) pixels above (below) the zero trend mark, indicating that drought prevails in both low and high elevation areas up to 2000 m. There was no direct link between ENSO and drought but arguably the association of drought in most El Niño and La Niña years suggests that the impact of ENSO cannot be ruled out since peak ENSO events occur during October to March periods which coincides with the short (SON) and long (MAM) rainy seasons of East Africa. The study is particularly relevant in being able to depict continuous and synoptic drought condition all over East Africa, providing vital information to farmers and policy makers, using very cost-effective method.

Keywords Meteorological Drought, Joint Probability Density Function (JPDF), SPI, ENSO, Drought Risk Mapping.

Introduction

Several studies indicate that droughts are among the most destructive natural disasters, negatively impacting livelihoods including crops and livestock, as well as other natural resources such as water, ecology, and biodiversity 2016 (Haroon et al., ; Lei et al., 2016; Schubert et al., 2016; Igbawua et al., 2018; Yao et al., 2018; Liu et al., 2020). The American Meteorological Society

(1997) categorizes droughts into meteorological, agricultural and hydrological mainly on the basis of duration, impact and recovery rate. According to Ghulam et al. (2007) and Haroon et al. (2016), meteorological drought refers to a sustained period of three months or more during which monthly precipitation remains well below the long-term average. Agricultural drought occurs when there is an imbalance between water availability and demand in a farmland ecosystem, where water demand by plants is more as compared to supply. Hydrological droughts occur when deficiencies in surface and subsurface water supplies become evident in terms of reduced stream flow and reduction in ground water. For the purpose of this study however, the assumption is that "drought occurs when precipitation deficit exceeds some critical level beyond which the prevailing adaptive mechanisms fail to cope", as defined by Tarhule and Woo (1997). The occurrence of drought has been recorded across all continents and under all climatic regions with low and high mean precipitation (Um et al., 2017) with varying degree, intensity, impact and duration. In recent decades, the occurrence and incidence of drought has been aggravated with the increase in global climate change (IPCC, 2014). For Africa, O'Connor (1995) reported that remotely sensed data analysis from National Aeronautics and Space Administration (NASA) reveal that about 900,000 km^2 of previous savanna grassland in the African region had been severely degraded between the early 1960s and 1986 due to persistent occurrences of drought, while Bates et al., (2008) estimated that one-third of African population live in drought-prone areas. Yang & Huntingford (2018) revealed historical precipitation estimated by Climate Hazards Group InfraRed Precipitation with Station data (CHIRPS) (Funk et al., 2015) shows that during August, September and October (ASO) of 2016, most of East Africa (particularly Somalia, Ethiopia and Kenya) had a reduction of 40% or more in precipitation compared to a baseline ASO period 1981–2015. Several studies confirm that the East African region ranks among the most vulnerable drought-prone regions of the world with a high potential for increased risk of drought related water and food shortages as recorded in as recent as year 2016/2017 (Love, 2009; Masih et al., 2014; Funk et al., 2014, 2015; Yang and Huntingford, 2018). The threat of drought is expected to further aggravate the existing widespread poverty and food insecurity (Funk et al., 2008, 2013, 2015; von Grebmer et al., 2016). The situation is similar within other regions of sub saharan Africa. In West Africa, Dai et al. (2004) reported that there is about 40% decline in annual precipitation total from the year 1968–1990 as compared with the 30 years between 1931 and 1960. Thus, frequent drought occurrences within the West African region have caused famine and are threatening the human existence in African savanna regions and consequently making the households highly vulnerable to drought (Eze, 2018).

Droughts are considered a ‘creeping’ disaster by nature with devasting and extended impact often requiring long periods to reverse the recorded damages. It is therefore crucial that consistent drought monitoring is carried out to provide decisive policy support for long- and medium-term planning of mitigative measures. Typically, at the turn of the 20th century, scientific studies had adopted climatic (temperature and precipitation) and hydrological (soil moisture and stream flow) indicators as main input towards the generation of indices for quantitative modelling of drought severity (Kincer, 1919; Munger, 1916; McQuigg, 1954; Waggoner and O'Connell, 1956). However, further advances in the study of drought (beginning from the latter part of the 20th century into the 21st century) led to the identification of over 150 indices used for drought studies (Niemeyer, 2008) across various regions with different climatic conditions. The most prominently adopted contemporary indices for drought research include, but not limited to: decile index (DI) by Gibbs and Maher (1967); Palmer drought severity index (PDSI) by Palmer (1968), standardized precipitation index (SPI) applied by McKee et al. (1993); reclamation drought index (RDI) by Weghorst (1996); US Drought Monitor (USDM) applied by Svoboda et al. (2002); optimized meteorological and vegetation drought indices (OMDI and OVDI) proposed by Hao et al. (2015); composite drought indices using multivariable linear regression (MCDIs) developed by Liu et al. (2020).

Recent drought studies have relied on the availability of data from different remote sensing platforms due largely to the synoptic coverage it provides for analysis over a wide region.

Numerous methods have been developed for the application of remotely sensed data in drought studies. These include normalized difference vegetation index (NDVI) based conceptualization such as vegetation condition index (VCI) (Kogan 1995), enhanced vegetation index (EVI) (Liu and Huete 1995), soil adjusted vegetation index (SAVI) (Huete 1988), temperature vegetation index (TVX) (Lambin and Ehrlich, 1995), Deviations from NDVI (Anyamba et al., 2001), vegetation health index (VHI) (Kogan, 2001), temperature condition index (TCI) (Kogan, 1995; Kogan et al., 2003), and temperature vegetation dryness index (TVDI) (Sandholt et al., 2002).

More advanced methods now include satellite derived indices such as perpendicular drought index (PDI) (Ghulam et al., 2007a); modified perpendicular drought index (MPDI) (Ghulam et al., 2007b); effective drought index (EDI) (Yao et al., 2010); and Drought severity index (DSI) proposed by Mu et al. (2013) and applied by Haroon et al. (2016).

For the purpose of this study, the SPI proposed by McKee et al. (1993), and applied in Indonesia by Pramudya and Onishi (2018) will be adopted for the analysis of drought across the East African region. The SPI is considered most applicable for this study because it provides for drought analysis in multi-temporal levels such as monthly, single seasonal, multi-seasonal, and annual basis. This level of spatio-temporal scale analysis allows for the SPI to provide accurate meteorological and agricultural drought analysis.

2.0 Methodology

2.1 Study Area

The study area covers eight countries consisting of Ethiopia, Kenya, Rwanda, Uganda, Tanzania, Burundi, Somalia and South-Sudan (Fig. 1). The climate of the region is influenced by a number of factors ranging from combination of the high altitude and the westerly monsoon winds that originate from the Ethiopian Highlands and Rwenzori Mountains. Generally, majority of the region's countries experience two distinct precipitation regimes: "long rains" which extend during March–May (MAM), and a season with "short rains", which lasts from October to December (OND). Figure 1 shows that much of Uganda and Somalia are humid and arid, respectively while much of Ethiopia is semi-arid and arid. South-Sudan and Tanzania are largely sub-humid, with Kenya containing a vast area of aridity. Rwanda and Burundi are largely tropical highlands. The major livelihood sources include pastoralism and agro-pastoralism, rangeland cultivation, small-holder agriculture, milk production and dairy products processing (Morton and Kerven, 2013; Abbink et al., 2014).

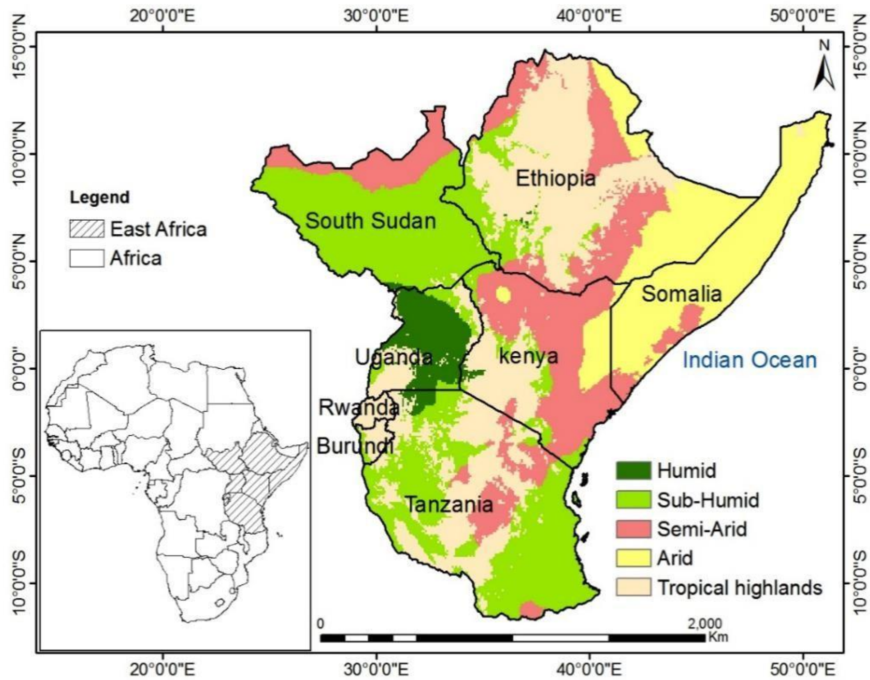

Fig. 1 Study area (Harvest Choice, 2015)

2.2 Data sets and methods

The precipitation data set used in this work is the Climate Research Unit (CRU) data developed by University of East Anglia. The data was retrieved from http://data.ceda.ac.uk/badc/cru/data/cru_ts/cru_ts_4.00/data/ at a spatial resolution of 0.5 x 0.5

degrees covering a temporal range of 1920 to 2015. The Standardized Precipitation Index (SPI) developed by McKee et al. (1993) is a popular index that is used to characterize drought at different time scales. SPI is computed by fitting a gamma distribution function to precipitation data of given frequency distribution over an area, and subsequently transforming the gamma distribution to a normal distribution with a mean and variance of zero (0) and one (1) respectively (Suryabhagavan, 2016). The aim of doing this is to minimize skewness in the data to zero. The Gamma distribution is widely used to represent precipitation time series (Guttman, 1999). The drought magnitude was obtained as the cumulative SPI over the drought months taken as a positive value. The intensity (drought severity) was computed as the magnitude divided by drought duration. The general technique for detecting changes in precipitation and drought is trend analysis. In this work, Trend analysis of precipitation and SPI will reveal will reveal the trends in drought over East Africa. Since, the input parameter for SPI computation is precipitation, trend analysis of precipitation will be done in order to study the local changes in climate. The Mann-Kendall non-parametric test was adopted in this work to assess the trends in precipitation and SPI and, also test the statistical distribution of the data records. Mann-Kendall was most preferred because it works well to avoid the problem caused by skewness of which precipitation is a kind of data that may be either negatively or positively skewed due to the existence of extreme values (Mahajan & Dodamani, 2015).

2.2.1 SPI

In calculating SPI, we adopt methods by Haroon, et al. (2016) and Guttman (1999), and fit a probability distribution to long-term monthly precipitation records. The mean $(\vec{x})$, standard deviation (s) and skew (sk) are determined as follows:

$$\text{mean } (\vec{x}) = \frac{\sum X}{N} \quad (1)$$

$$\text{standard deviation (s)} = \sqrt{\frac{\sum (X-\vec{X})^2}{N}} \quad (2)$$

$$\text{skewness (sk)} = \frac{N}{(N-1)(N-2)} \cdot \frac{\sum (X-\vec{X})^2}{N} \quad (3)$$

where, x is the precipitation time series and N is the length of data records. The precipitation data are transformed by the log normal (ln) and the mean of those values is computed. The transformed values are further subjected to the constant U, which is used to compute the shape and Scale parameter as follows:

$$\text{Log mean} = \vec{X}_h = \frac{\ln (X)}{N} \quad (4)$$

$$U = \ln (X) - \frac{\ln (X)}{N} \quad (5)$$

$$\text{Shape } (\beta) = \frac{1}{4U}\left[1 + \sqrt{\frac{4U}{3}}\right] \quad (6)$$

and,

$$\text{Scale } (\alpha) = \frac{\vec{X}}{\beta} \quad (7)$$

Further, the log values are transformed by the gamma distribution, incorporating the shape and scale values:

$$\text{Cumulative Gamma function } G(x) = \frac{1}{\alpha^{\beta}\Gamma\beta}\int_{o}^{x} x^{\beta-1} e^{-\frac{x}{\alpha}} dx \quad (8)$$

Similarly, $t = \sqrt{\ln\left(\frac{1}{(1-X_g)^2}\right)}$, where $0.5 < X_g \leq 1.0$

and, we perform T transform as $= \sqrt{\ln\left(\frac{1}{X_g^2}\right)}$, where $0 < X_g \leq 0.5$ (9)

and the SPI= $-\left(t - \frac{C_0 + C_1 t + C_2 t^2}{1 + d_1 t + d_2 t^2 + d_3 t^3}\right)$ where $0 < X_g \leq 0.5$ (10)

or SPI= $t - \frac{C_0 + C_1 t + C_2 t^2}{1 + d_1 t + d_2 t^2 + d_3 t^3}$ where $0.5 < X_g \leq 1.0$ (11)

The constants expressed in equations (10) and (11) are given as follows

C_0=2.515517, d_1= 1.432788

C_1=0.802853, d_2= 0.189269

$C_2 = 0.010328$, $d_3 = 0.001308$

2.2.2 Drought Magnitude, Duration and Intensity

The drought magnitude (D_M) was obtained as follows

$$D_M = -\sum_{i=1}^{n} SPI_{ij} \quad (12)$$

where D_M is the drought magnitude, n is the number of months with drought event at j timescale.

Drought intensity (D_I) is the ratio of drought magnitude (D_M) to drought duration (D_d) as follows:

D_M

$$D_I = \frac{\quad}{Dd} \qquad (13)$$

2.2.3 Mann-Kendall Trend Test

The Mann-Kendall trend test is given as

$$S = \sum_{i=1}^{n-1}\sum_{j=i+1}^{n} sgn(x_j - x_i) \qquad (14)$$

where x_i is the time series ranked from i= 1, 2,………n-1 and x_j from $j=i$+1,2,……..n. All the data values are taken as reference point to which comparison is done with the rest of the data values x_j such;

$$sgn(x_j - x_i) = \begin{cases} +1, > (x_j - x_i) \\ 0, = (x_j - x_i) \\ -1, < (x_j - x_i) \end{cases} \qquad (15)$$

The statistics of variance is given as

$$Var(S) = \frac{n(n-1)(2n+5) - \sum_{i=1}^{m} t_i(i)(i-1)(2i+5)}{18} \qquad (16)$$

where t_i is the number of ties up to sample value i. Z_c is the test statistics and is calculated as $Z_c =$

$$\begin{cases} \frac{S-1}{\sqrt{Var(S)}}, S > 0 \\ 0, \quad S = 0 \\ \frac{S-1}{\sqrt{Var(S)}}, S < 0 \end{cases} \qquad (17)$$

Z_c describes a Standard Normal Distribution (SND) and positive and negative values of Z_c shows an upward and downward trend respectively. According to Mondal et al. (2012), a significance level is also used in testing either an upward or downward monotone trend, if γ Z_c is greater than $Z_{\gamma/2}$ then the trend is considered significant and vice versa.

2.2.4 Sen's Trend Estimator

The Sen's trend estimator test was described by Sen (1968) and the magnitude of the trend is given by

$$T_i = \frac{x_j - x_k}{j - k} \quad (18)$$

where x_j and x_k are considered as data points j and k (j>k) compatibly. The median of these N values of T_i is represented as Sen's estimator of slope which is given as

$$Q_i = \begin{cases} T_{\frac{N+1}{2}} & N \text{ is odd} \\ \frac{1}{2}\left(T_{\frac{N}{2}} + T_{\frac{N+2}{2}}\right) & N \text{ is even} \end{cases} \quad (19)$$

Positive and negative values of Q_i represent upward (increasing) and downward (decreasing) trends, respectively.

In order to assess the spatio-temporal occurrence of drought over East Africa, the 3-month, 6-month and 12-month SPI was used to study drought in the long term. This period is enough for drought frequency and intensity assessment. The SPI was computed on monthly scale so that the consistency of drought duration and intensity can be determined according to Table 1.

Table 1 Standard SPI table (McKee et al., 1993)

SPI value	Description
2 >	Extremely wet
1.5 – 1.99	Very wet
1.0 – 1.49	Moderately wet
0 – 1.0	Mildly wet
-1.0 – 0	Mildly drought
-1.5 – -1.0	Moderately drought
-2.0 – -1.5	Severe drought
-2 <	Extreme drought

From a statistical point of view, droughts are considered as multivariate events whose dimension and treatment depends on their characteristics such as the duration, severity and frequency (Gonzalez et al., 2004). Most studies have proposed the Joint Probability Distribution Function (JPDF) for determining probabilistic characteristic because drought severity and duration are often difficult to treat separately.

Given a set of observations y_i........y_n, a mathematical expression of bivariate Kernel probability density estimator f_{SD} is given as (kim et al., 2003):

$$f_{SD}(s,d) = \frac{1}{n h_s h_d} \sum_{i=1}^{n} \left\{ K\left(\frac{S-S_i}{h_s}\right) K\left(\frac{d-d_i}{h_d}\right) \right\} \qquad (20)$$

The joint return period of drought (T_{Sd}) is given as (kim et al., 2003):

$$T_{Sd} = \frac{N}{n[1 - f_{SD}(s,d)]} \qquad (21)$$

where N is the numbers of years.

3. Results

3.1. Seasonal Characteristics of Precipitation and Precipitation Anomaly over East Africa from 1920 to 2015

The seasonal characterization of precipitation over the East African region (Fig. 2) reveals that long precipitations occur during the period of March to May (MAM) while short precipitations occur from the period of October to December (OND). The study analysis revealed that peak annual precipitation from 1920 to 2015 is recorded as 120 mm/yr while average seasonal cumulative precipitation from 1920 to 2015 is about 920 mm/yr. Crop production over East Africa is highly dependent on the long rainy season, which accounts for more than 70% of total annual precipitation. It is therefore, understandably that fluctuations in precipitation within this period is capable of altering and impacting food production across the region.

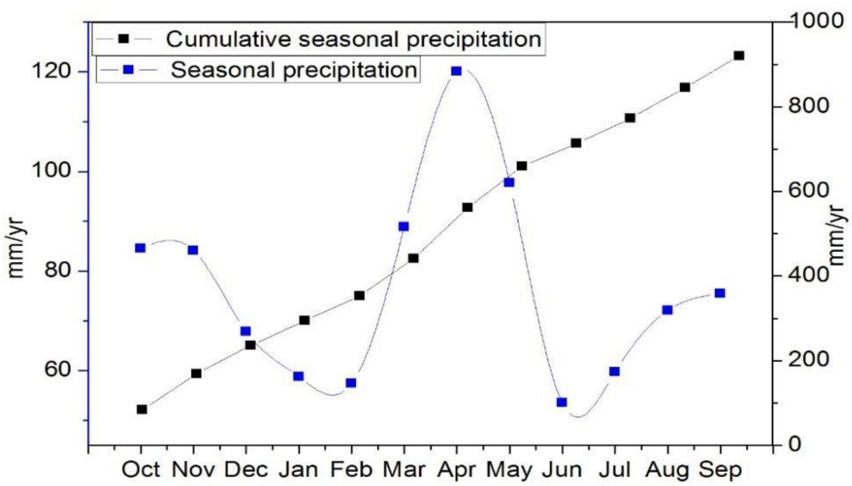

Fig. 2 Characteristics of precipitation over East Africa

Figure 3 shows precipitation anomalies from 1920 to 2015. Positive and negative anomalies represent wet and dry conditions, respectively, over East Africa. Based on the data used from 96 years (from 1920 to 2015) there are a total of 41 wet years and 46 drought years. The anomaly of the wet years and dry years were obtained when precipitation was above and below normal conditions, respectively, as seen in Fig. 3. The years 1961, 1967, 1997, 2007 and 2015 are the wettest while 1943, 1983, 1993, 1997 and 2003 are the driest. The annual precipitation, anomalies and the corresponding SPI's for wet and dry years are presented in Table 2. Results show that both wet and drought spells coincide with positive and negative anomalies over East Africa, respectively. This shows that the reason for the drought periods was as a result of unavailability of water in the soil. The magnitude of anomaly of the wet years was higher than that of the dry years and both wet and dry years were obtained when precipitation was above and below normal conditions, respectively. A detailed inspection of dry- and wet-year results also revealed that the chances of occurrence of wet years are greater in comparison to dry years. This information is important for the future planning and management of agricultural practices. This work has allowed us to identify years within the region that are prone to dry/wet conditions using available precipitation data records from 1920 to 2015.

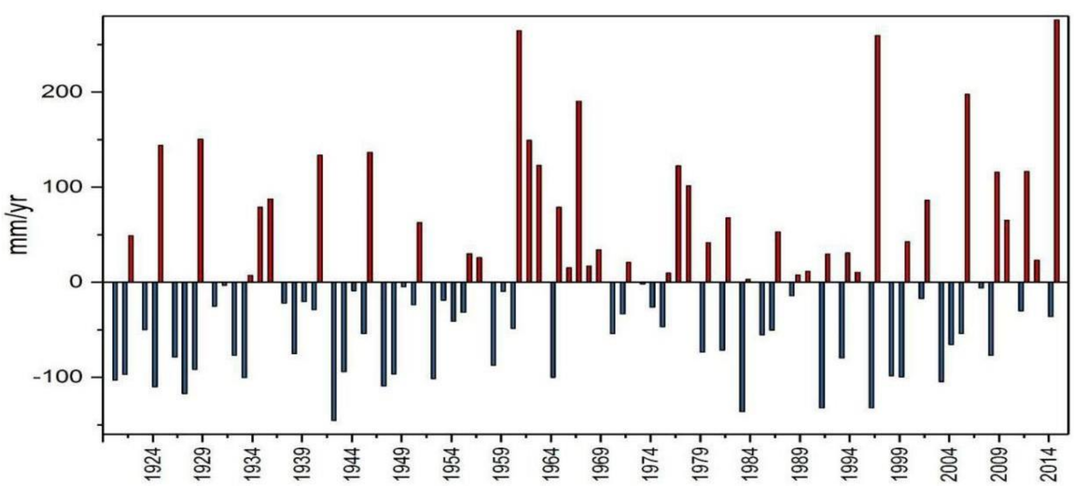

Fig. 3 Precipitation anomaly over East Africa

Table 2 Annual precipitation, anomaly and SPI-12

Condition	Yr	Annual precipitation (mm/yr)	Anomaly (mm/yr)	SPI
	1920-21	817.7	-102.8	-1.2
	1921-22	823.5	-96.9	-1.1
	1924-25	810.4	-110.0	-1.2
	1927-28	803.3	-117.2	-1.3
	1928-29	828.7	-91.7	-1.0
	1933-34	820.1	-100.3	-1.1
	1942-43	775.0	-145.4	-1.7*
Dry Spells	1943-44	826.4	-94.1	-1.0
	1947-48	811.3	-109.1	-1.2
	1948-49	823.7	-96.7	-1.1
	1952-53	818.9	-101.5	-1.1
	1964-65	820.4	-100.0	-1.1
	1983-84	784.2	-136.2	-1.6*
	1991-92	788.1	-132.3	-1.5*
	1996-97	788.2	-132.2	-1.5*
	1999-00	820.7	-99.7	-1.1
	2003-04	815.8	-104.7	-1.2

	Yr	Annual precipitation (mm/yr)	Anomaly (mm/yr)	SPI
	1925-26	1064.5	144.1	1.6
	1929-30	1071.0	150.6	1.6
	1941-42	1054.0	133.6	1.4
	1946-47	1056.9	136.5	1.5
	1961-62	1185.0	264.5	2.7**
	1962-63	1069.6	149.2	1.6
	1963-64	1043.2	122.8	1.3
	1967-68	1110.8	190.4	2.0**

Wet Spells	1977-78	1042.9	122.4	1.3
	1978-79	1021.9	101.5	1.1
	1997-98	1180.0	259.6	2.7**
	2002-03	1006.7	86.3	1.0
	2006-07	1118.2	197.8	2.1**
	2009-10	1036.0	115.6	1.3
	2012-13	1036.8	116.4	1.3
	2015-16	1196.4	275.9	2.8**

3.2. Spatial and temporal representation of spatial SPI over East Africa

Figure 4 shows the spatial representation of SPI for different hydrological years from 1920 to 2015 over East Africa. Results show that Figs. 4a, d and k recorded the highest precipitation while Fig. 4b, e and h recorded the least precipitation. It is critical to note that most of the regions that recorded the highest precipitation in some years also recorded the least in other years, hence establishing the fact that precipitation across most of the East African region is fluctuating and drought is not peculiar to one region.

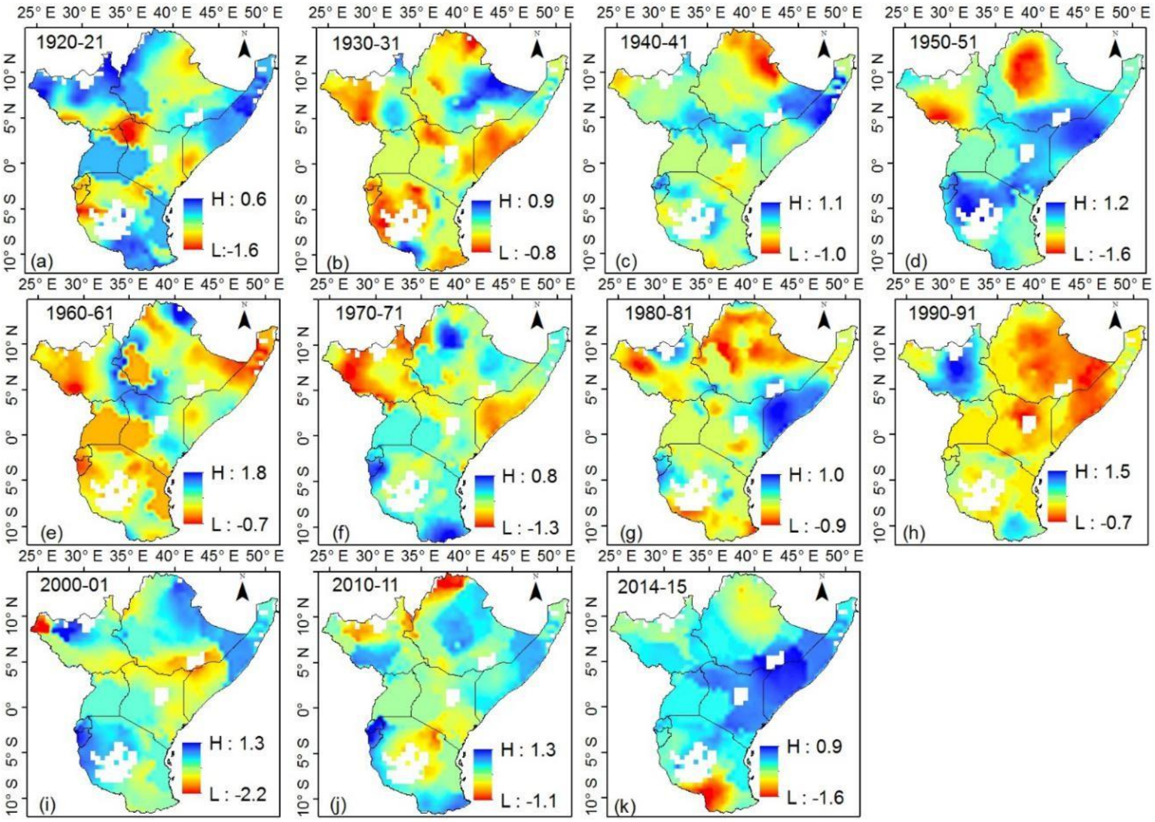

Fig. 4 Spatial representation of SPI for different hydrological years over East Africa

From Fig. 5, calculated SPI at different time scales of 3, 6 and 12 months indicated that for shorter time scales (i.e., 3 months, 6 months), there was a high temporal variability in dry and wet periods, whereas at longer time scales (12 months), frequency of dry and wet periods were considerably decreased.

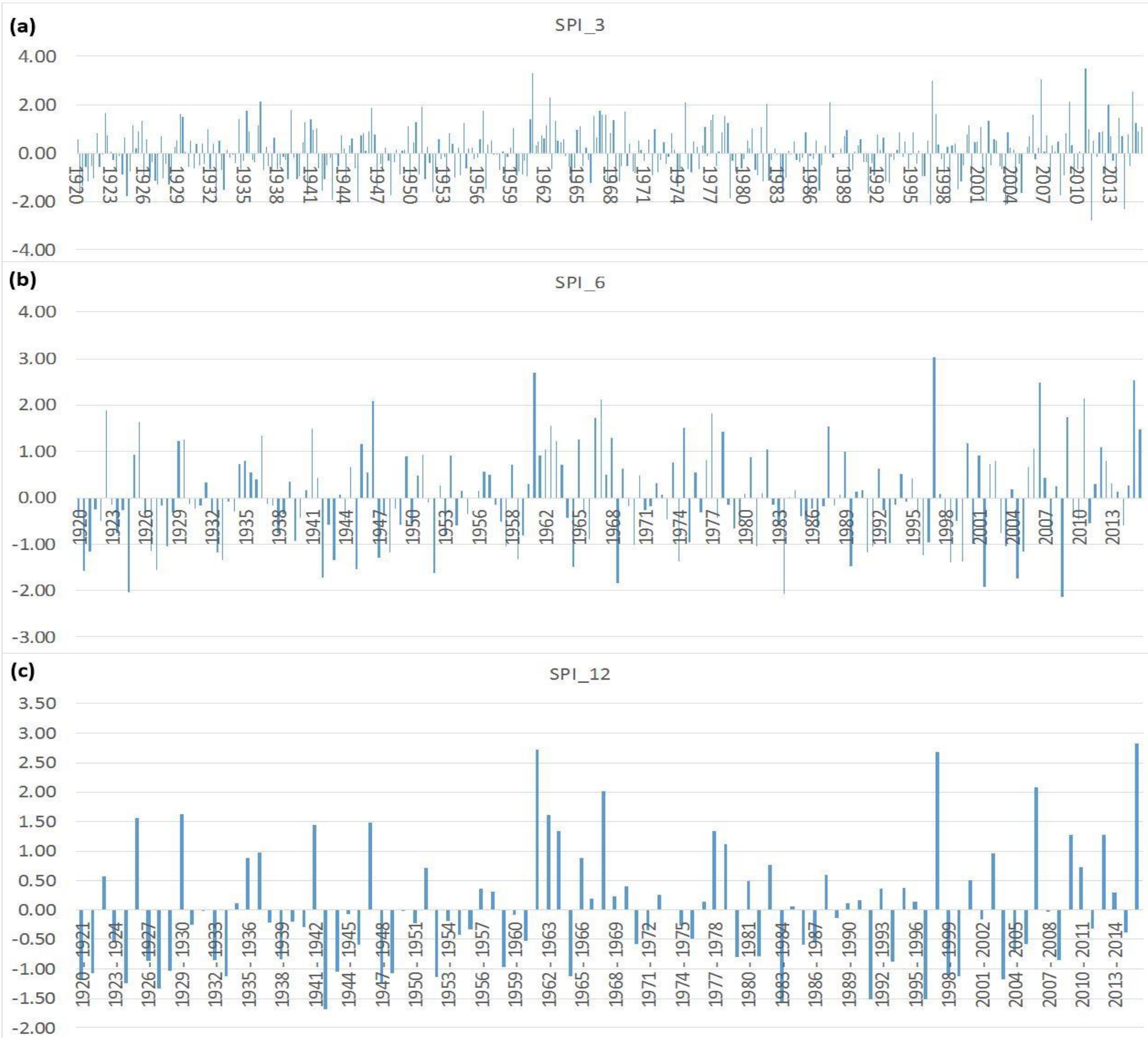

Fig. 5 (a) SPI-3 months (b) SPI-6 months (c) SPI-12 months

The drought magnitude, drought duration, and corresponding drought intensity were calculated over the study area (Table 3). And also, Fig. 6 shows drought magnitude over east Africa. Years with high drought magnitude ranged from 1922-22, 1926-29, 1942-46 and 1947-51 with values corresponding to 2.2, 3.2, 3.4 and 2.6, respectively while years with low drought magnitude ranged from 1930-31, 1988-89 and 2001-02 with values as 0.2, 0.12 and 0.15, respectively. Figure 7 shows drought duration in years over East Africa with the longest droughts occurring from 1929-29, 1937-41, 1942-46, 1947-51, 1952-56, and 1958-61 with values in years as 3, 4, 4, 4, 4, and 3 years, respectively, while the shortest droughts occurred in time period of 1 year and ranged from 1930-31, 1964-65, 1979-80, 1981-82, 1983-84, 1988-89, 1991-92, 1993-94, 1996-97 and 2001-02 (Also see Table 3). A comparison between Fig. 6 (drought magnitude) and Fig. 7 (drought duration) shows that not all the severest drought took longer and vice versa. Both drought magnitude and duration showed a negative slope of -0.071 and -0.086, respectively.

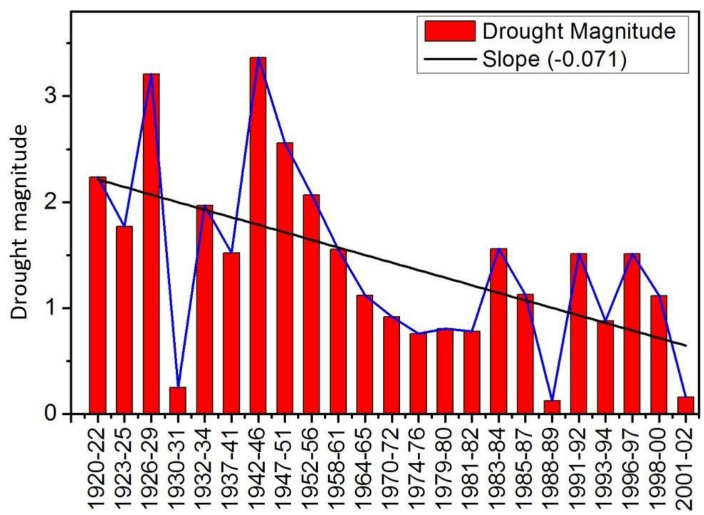

Fig. 6 Drought magnitude over East Africa

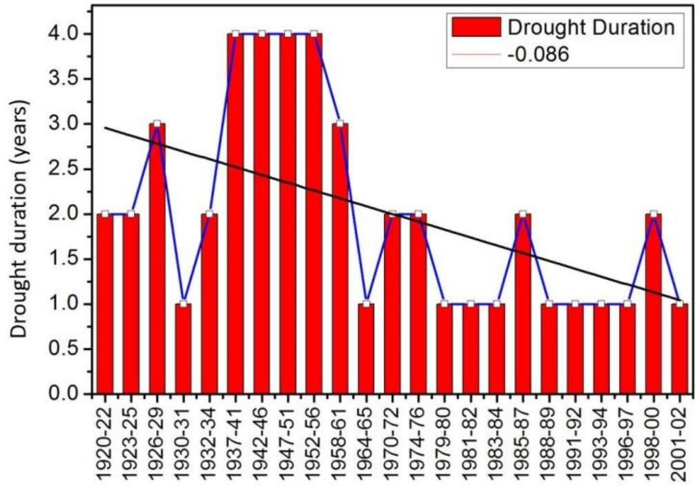

Fig. 7 Drought duration over East Africa

The drought magnitude was obtained as the cumulative SPI over the drought months taken as a positive value. The intensity (drought severity) was computed as the magnitude divided by drought duration. Among the droughts recorded, the drought of 1937-41, 1942-46, 1947-51, 1952-56 had the longest duration. Specifically, the results indicated that on one hand the frequency of drought events were high at shorter time scales but lasted for shorter durations at longer time intervals, and on the other hand droughts were less frequent but persisted for longer periods of time.

Table 3 Extraction of drought characteristics

Hydrological year	Magnitude	Duration	Intensity
1920-22	2.2333	2.000	1.1167
1923-25	1.7703	2.000	0.8852
1926-29	3.2102	3.000	1.0701
1930-31	0.2493	1.000	0.2493
1932-34	1.9668	2.000	0.9834
1937-41	1.5215	4.000	0.3804
1942-46	3.3653	4.000	0.8413
1947-51	2.5589	4.000	0.6397

1952-56	2.0666	4.000	0.5166
1958-61	1.5564	3.000	0.5188
1964-65	1.1191	1.000	1.1191
1970-72	0.9154	2.000	0.4577
1974-76	0.7563	2.000	0.3781
1979-80	0.8044	1.000	0.8044
1981-82	0.7803	1.000	0.7803
1983-84	1.5593	1.000	1.5593
1985-87	1.1279	2.000	0.5640
1988-89	0.1257	1.000	0.1257
1991-92	1.5109	1.000	1.5109
1993-94	0.8771	1.000	0.8771
1996-97	1.5102	1.000	1.5102
1998-00	1.1151	2.000	0.5576
2001-02	0.1588	1.000	0.1588

Figure 8 shows the spatial map of drought magnitude across the East African region for different hydrological years.

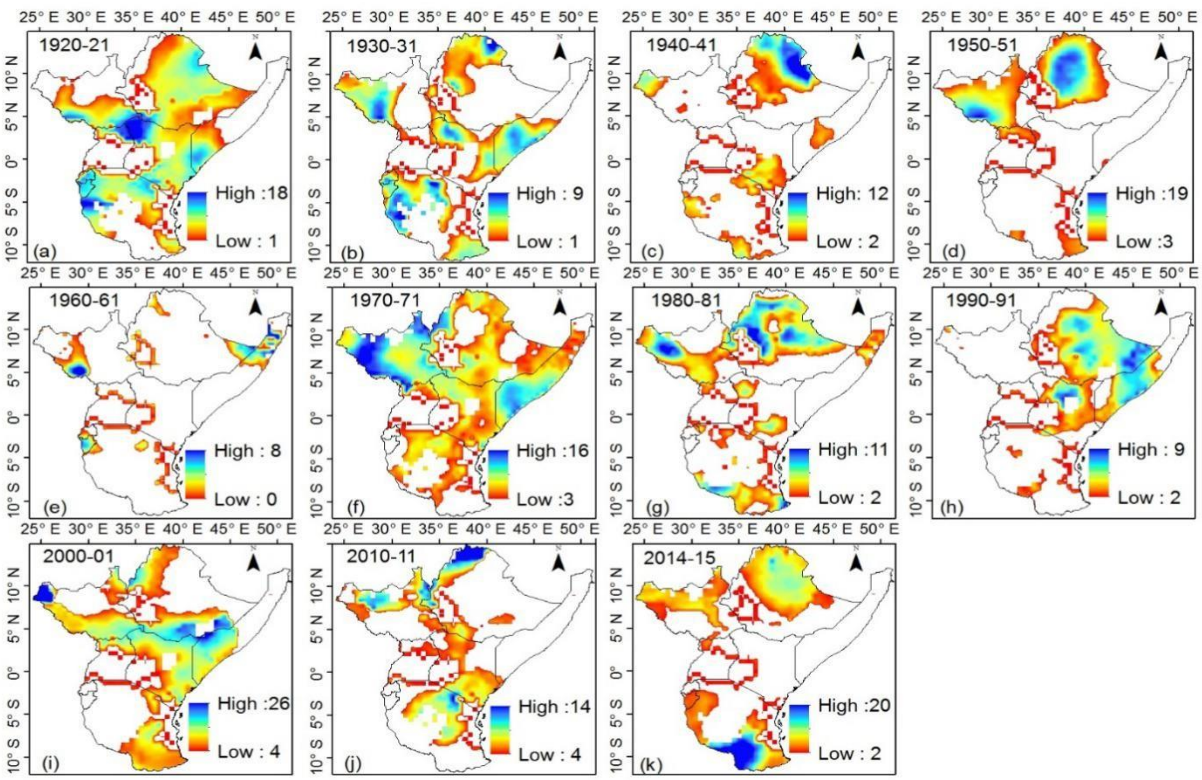

Fig. 8 Spatial drought magnitude over East Africa for different hydrological years

The results show that the drought magnitude is highest in 1920-21, 1950-51, 1970-71, 2000-01 and 2014-15 hydrological years. In 1920-21 hydrological year, regions that recorded high drought magnitude include South Sudan, Uganda, Kenya, Rwanda, Burundi and Eastern Tanzania. In 1950-51hydrological year, drought magnitude was highest over Ethiopia and South Sudan. In 1970-71 hydrological year, drought magnitude was highest over South Sudan, Ethiopia and Somalia. In 2000-01 hydrological year, drought magnitude was highest in South Sudan, Ethiopia, Somalia and Kenya. In 2014-15 hydrological year, drought magnitude was highest in Ethiopia and

Tanzania. This indicated that besides seasonal variability of spatial drought magnitude, there exist a strong variability of spatial drought magnitude across different decades.

3.3. Drought Risk Mapping and Joint Probability Distribution Function and Return years of Drought over East Africa

The spatial drought risk map was got from the spatial SPI map and represented in Fig. 9. It shows the spatial drought levels over East Africa across different decades, and changes across the region's land mass suggested to be as a result of changes in climate and land cover. There is high variability in drought across the decades over the region. These droughts could be categorized as ranging from moderate to extreme, with different durations and magnitudes. Nevertheless, the total duration, severity and magnitude of occurrence of the drought episodes varied from one location to another across the decades.

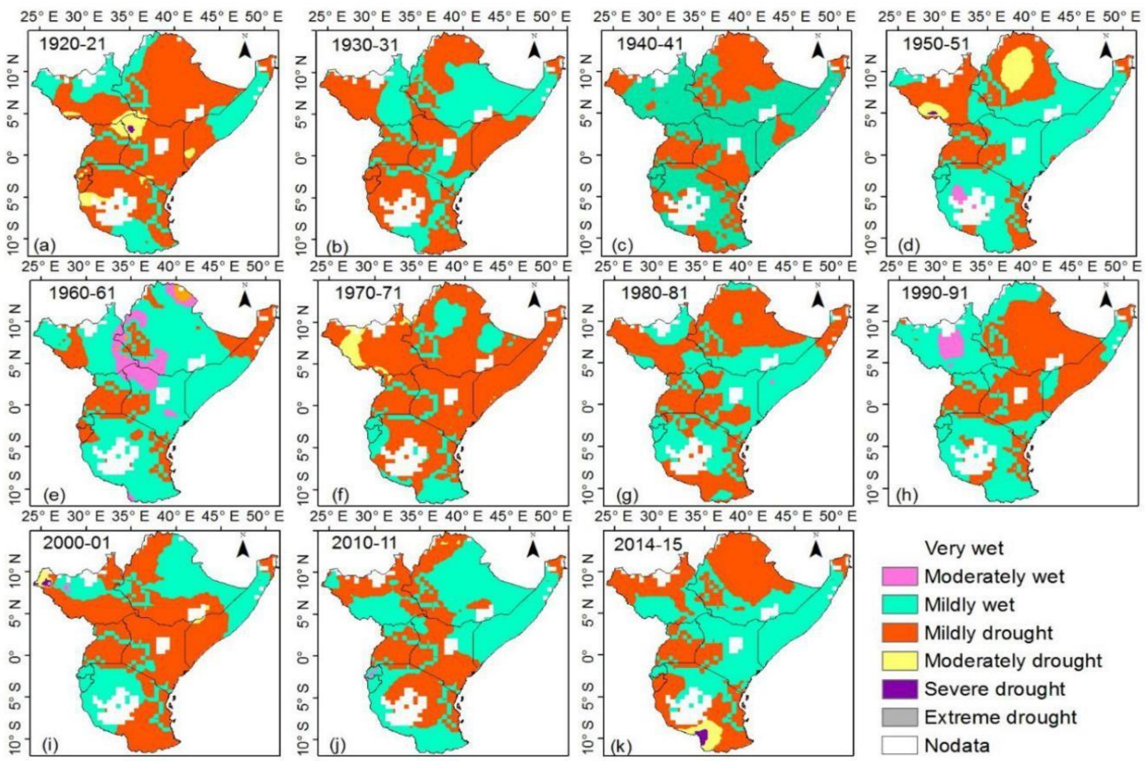

Fig. 9 The spatial drought risk map across East Africa

From Fig. 9, it appears as if drought repeats itself in some selected locations after a period of time but all droughts experienced in all locations and at all recorded periods appear to differ (see Figs. 9a to 9k). Drought may have similar magnitudes or duration but different levels of severity.

For example, the droughts with magnitude (duration in years) of 1.5(4), 3.4(4), 2.6(4) and 2.0(4) lasted from 1937 to 1941, 1942 to 1946, 1947 to 1951 and 1952 to 1956, respectively (see Table 3). Since both drought severity and durations have different distributions, the Joint Probability Distribution Function (JPDF) given by equation (9) was used to obtain the probability Density function and the Joint return years were obtained using equation (10). The JPDF analysis is a useful multivariate tool needed for water resources management. Based on the drought characteristics, duration and magnitude using the 12-month SPI, the JPDF was estimated as shown in Figure 10.

From Fig.10, it shows that probability of drought occurrence is high when severity is low and such droughts occur at short time intervals. Also, it takes so many years for a severe drought to repeat itself at short time intervals.

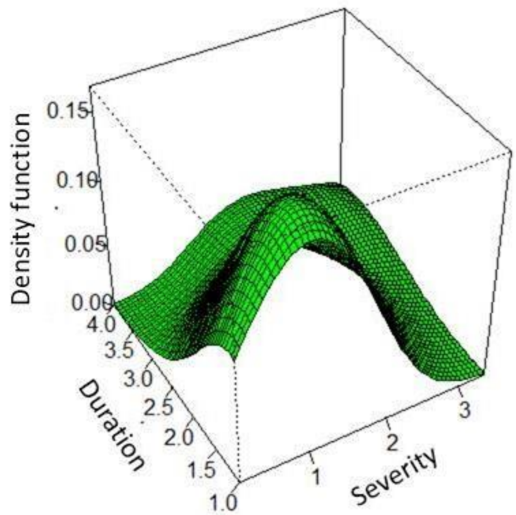

Fig.10 The JPDF for drought duration and severity (magnitude)

Once the JPDF for the bivariate return periods of drought was calculated, the drought severity duration frequency curve of East Africa was created (Fig.11). Fig.11 is a bivariate analysis of drought severity for East Africa region showing return periods and different levels of severity.

Drought severity itself is a function of the different drivers of drought over particular area. Drought severity characterizes drought magnitude of dry events. The JPDF drought-based curves were developed for selected recurrence severity levels of 5, 10, 20, 30, 40 and 50 years are plotted in Fig.11. It is observed that for any given duration, severe droughts have more return periods.

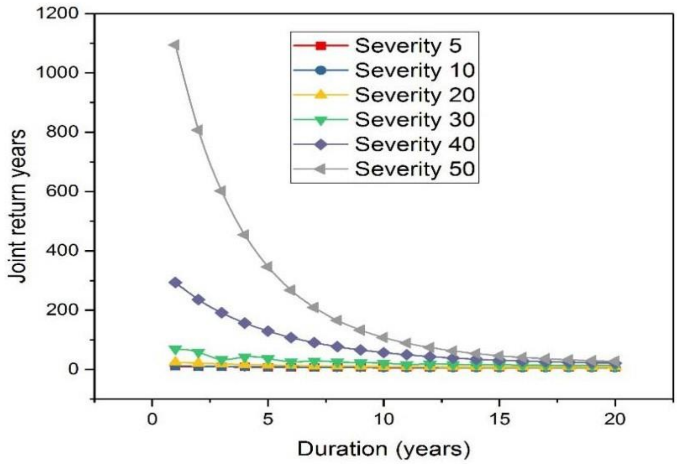

Fig. 11 Joint return years for severity (magnitude) corresponding to duration

Table 4 shows the drought occurrence over East African countries. The result shows that the drought mechanism is complex and the drivers highly depend on the local environmental conditions prevailing in a particular country. All drought episodes are associated with negative precipitation anomalies, low precipitation values closely matching the SPI values. The SPI values depicting drought levels (shown in Table 1) are applied to reveal the varying levels of drought experienced over specific countries in East Africa over the study period.

Table 4 Annual precipitation anomalies for various countries in East Africa from 1920-2015 with SPI-12. The value in parenthesis represents SPI

	Burundi	Rwanda	Ethiopia	Kenya	Somalia	Uganda	Tanzania	South Sudan
1920/21	-145 (-1.0)	-197 (-1.3)				-188(-1.4)		
1921/22	-383 (-3.0)							
1923/24	-174 (-1.2)	-231 (-1.5)						
1924/25			-93 (-1.0)	-150 (-1.2)		-190 (-1.4)	-165 (-1.3)	-84 (-1.0)
1926/27						-168 (-1.2)		-106 (-1.3)

1927/28	-259 (-1.9)	-225 (-1.5)		-125 (-1.0)		-155 (-1.1)		
1928/29	-216 (-1.6)	-158 (-1.0)		-128 (-1.0)		-144 (-1.0)	-191 (-1.5)	
1932/33			-96 (-1.1)	-163 (-1.4)				
1933/34	-285 (-2.1)	-291 (-2.0)				-163 (-1.2)		
1938/39			-95 (-1.0)		-72 (-1.0)	-191 (-1.4)		
1940/41			-102 (-1.1)					
1942/43	-203 (-1.5)	-237 (-1.6)	-146 (-1.7)	-129 (-1.0)		-215 (-1.6)		-123 (-1.5)
1943/44		-158 (-1.0)			-109 (-1.7)	-139 (-1.0)	-128 (-1.0)	
1945/46		-165 (-1.1)			-104 (-1.6)		-193 (-1.5)	
1947/48	-199 (-1.4)		-89 (-1.0)	-128 (-1.0)	-122 (-2.0)			
1948/49					-88 (-1.3)		-241 (-2.0)	
1950/51			-170 (-2.0)					-124 (-1.5)
1952/53			-100 (-1.1)			-177 (-1.3)	-222 (-1.8)	
1953/54					-72 (-1.0)			
1954/55					-106 (-1.6)			
1955/56			-130 (-1.5)		-117 (-1.8)			
1958/59	-193 (-1.4)				-68 (-1.0)		-162 (-1.3)	
1960/61	-211 (-1.5)	-148 (-0.9)					-164 (-1.3)	
1964/65			-121 (-1.4)	-140 (-1.2)	-80 (-1.2)	-213 (-1.6)	-148 (-1.1)	
1970/71					-86 (-1.3)			-99 (-1.2)
1971/72								-132 (-1.6)
1975/76				-183 (-1.6)				
1979/80			-113 (-1.3)	-149 (-1.2)	-77 (-1.1)	-189 (-1.4)		-110 (-1.3)
1981/82		-157 (-1.0)						-121 (-1.5)
1982/83								-125 (-1.5)
1983/84			-151 (-1.7)	-248 (-2.2)	-83 (-1.2)	-177 (-1.3)		-228 (-2.9)
1985/86			-114 (-1.3)					
1986/87			-105 (-1.2)					-218 (-2.8)

1989/90								-124 (-1.5)
1991/92	-144 (-1.0)	-151 (-1.0)	-155 (-1.8)	-147 (-1.2)	-156 (-2.7)	-154 (-1.1)		-97 (-1.2)
1993/94	-161 (-1.1)				-84 (-1.2)		-137 (-1.0)	
1996/97	-152 (-1.1)		-138 (-1.6)	-136 (-1.1)	-90 (-1.3)	-160 (-1.2)	-169 (-1.3)	-86 (-1.0)
1998/99		-166 (-1.1)	-104 (-1.2)	-171 (-1.4)	-87 (-1.3)			
1999/00	-158 (-1.1)	-209 (-1.4)		-161 (-1.3)			-254 (-2.1)	
2003/04		-250 (-1.7)	-141 (-1.6)	-161 (-1.3)		-177 (-1.3)		
2004/05				-160 (-1.3)		-178 (-1.3)		
2005/06		-175 (-1.1)					-139 (-1.1)	
2007/08						-142 (-1.0)		
2008/09								-150 (-1.9)
2010/11				-119 (-1.0)			-150 (-1.2)	
2011/12	-204 (-1.5)							

Note: 1920/21 represents a hydrological year starting in 1920 and ending in 1921.

The spatial and temporal variability in drought trends is observed in the study area and shown in Table 5 as the Negative and Positive SPI trends at multiple time scales across the East African countries. Of all the SPI models tested, only SPI-12 indicated significant trend values in Burundi, Rwanda and Uganda with Sen's slope (Kendal tau) values of 0.008 (0.143), 0.007 (0.144) and 0.008 (0.149) respectively. Basically, the SPI-12 shows the status of year-round water shortage caused by drought while SPI-6 and SPI-3 are appropriate indicators of the status of seasonal water shortage caused by drought (Tan et al., 2015).

Table 5 Mann-Kendall Trend and significance level of SPI-3, SPI-6 and SPI-12 over East African countries

Duration	Parameter	Burundi	Ethiopia	Kenya	Rwanda	South Sudan	Somalia	Tanzania	Uganda	Regional

SPI-3	Kendal τ	0.060	0.017	-0.004	0.089	-0.058	0.026	-0.028	0.062	0.036
	(Sign)	(0.086)	(0.635)	(0.914)	(0.011)	(0.097)	(0.450)	(0.419)	(0.074)	(0.307)
	Sen's slope	0.002	0.004	-0.0001	0.003	-0.005	0.002	-0.003	0.0002	-0.0001
	Trend	No	No	No	No	No	No	No	No	No
SPI-6	Kendal τ	0.073	0.008	0.006	0.087	-0.051	0.040	-0.057	0.087	0.037
	(Sign)	(0.140)	(0.879)	(0.908)	(0.079)	(0.305)	(0.421)	(0.247)	(0.079)	(0.457)
	Sen's slope	0.004	0.0001	-0.0003	0.004	-0.003	0.002	-0.003	0.005	0.002
	Trend	No	No	No	No	No	No	No	No	No
SPI-12	Kendal τ	0.143	-0.009	0.031	0.144	-0.071	0.072	-0.016	0.149	0.103
	(Sign)	(0.040)	(0.903)	(0.662)	(0.039)	(0.301)	(0.301)	(0.817)	(0.033)	(0.141)
	Sen's slope	0.008	-0.001	0.001	0.007	-0.004	0.004	-0.001	0.007	0.006
	Trend	Yes	No	No	Yes	No	No	No	Yes	No

Table 6 shows negative and positive precipitation trends at multiple time scales over East African countries. Out of eight countries, precipitation shows significant positive (insignificant positive) trends over 1(4) countries and significant (insignificant) negative trends over 1(2) countries from 1920 to 2015.

Table 6 Mann-Kendall Trend and significance level of precipitation over East African countries

Country	Kendal τ (sign)	Sen's slope	Trend
Burundi	0.023 (0.248)	0.021	No
Ethiopia	-0.001 (0.980)	-0.034	No
Kenya	0.005 (0.799)	0.006	No
Rwanda	0.034 (0.088)	0.092	No
South-Sudan	-0.044 (0.028)	-0.042	Yes
Somalia	0.048 (0.05)	0.007	Yes
Tanzania	-0.010 (0.603)	-0.010	No
Uganda	0.033 (0.101)	0.022	No
Regional	0.025 (0.216)	-0.005	No

3.4 Spatial trends in drought across East Africa

Figure 12 shows the spatial trend of SPI over East Africa. The approach involves running an Ordinary Linear Regression model to the SPI maps generated. Results show that about 28, 22 and 50 % of the SPI indicated spatial increase, no change and decrease in SPI trends respectively over the study area from 1920 to 2015. Increase (decrease) of SPI trends by our analysis means an increase (decrease) in moisture conditions corresponding to decrease (increase) in drought prevalence. Assessing the mean SPI drought characteristics over the region indicates that there were some notable variations in SPI, consistent with the distribution of precipitation. Areas with increase in SPI were located northeast, along the shores of the Indian Ocean and some few areas in the Central part of the study area. Areas with no trend changes in SPI were located in northwest, northeast, southeast parts of East Africa and close to the shores of the ocean. Also, areas with decreasing SPI trend pixels were located around in the Northwest, Northeast, and Southwest and along the shores of the study area. The 96-year precipitation records in areas with spatial increase in SPI trend were 11.3, 136.5, 77.3 and 26.5 mm for minimum, maximum, mean and standard deviation values respectively while the precipitation records in areas with spatial decrease in SPI were 539, 138.3, 56.1 and 29.7 for minimum, maximum, mean and standard deviation values respectively. For areas with no spatial trend changes in SPI were 7.2, 161.6, 93.2 and 31.9 for minimum, maximum, mean and standard deviation values, respectively. Areas with improvement in drought indicated the low precipitation standard deviation. Our result confirms that areas with no SPI changes in drought were wetter from 1920 to 2015.

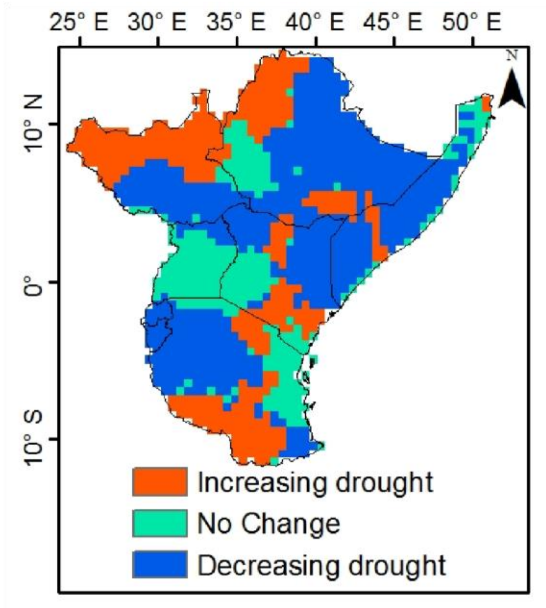

Fig.12 Spatial trends in SPI over East Africa

Figure 13a shows the spatial slope of SPI versus latitudes (degrees). Results indicate that high of SPI slope are clustered at higher latitudes from ^{o}latitude 0 to 12 while low trend values are clustered between ^{o} latitude -2 and 2 south of the study region which is an indication that drought is prevalent in the northern section than southern section of the study area.

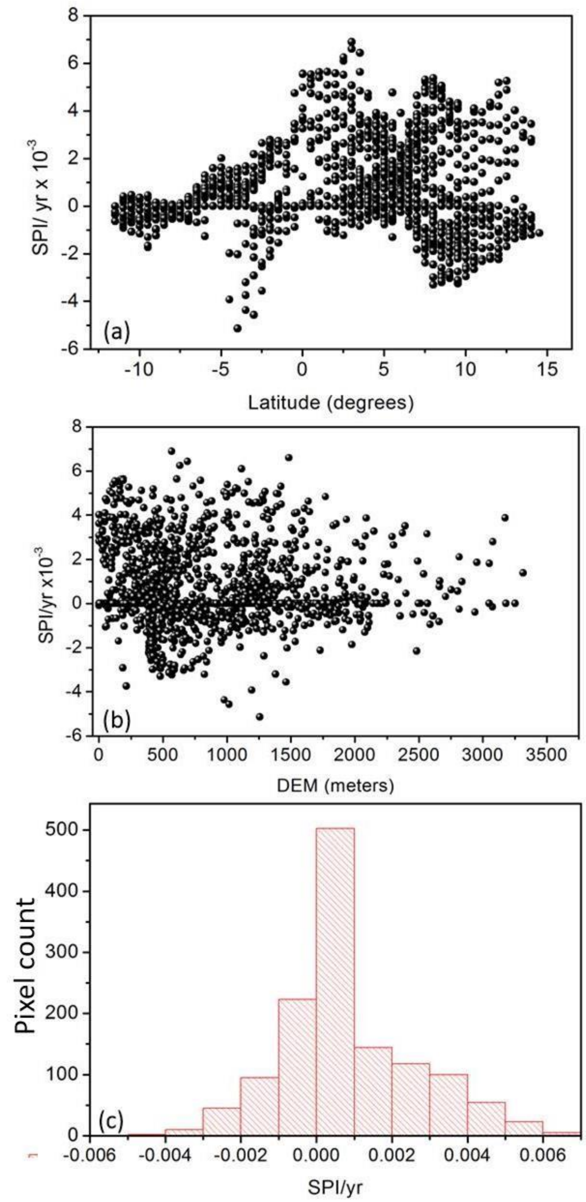

Fig.13 (a) SPI slope versus latitude (b) SPI slope versus DEM and (c) histogram of pixel count

Figure 13b shows SPI slope versus DEM where both high and low slope values of SPI are clustered at lower latitudes between 0 to 1500 m, and at the foot hills of mountains. The histogram of the SPI trends is shown in Figure 13c. It can be observed that most of the SPI trends are clustered around the 0.0 mark, which shows that the density curve of the pixels is symmetrical and centered about its mean. The SPI trends indicate high positive (negative) pixels above (below) the zero trend mark, implying that drought prevails in both low and high elevation areas up to 2000 m.

3.5 ENSO-drought relationship

Drought is considered as one of the most complex and deleterious natural, with severe impacts on natural ecosystems, water resources and food security (Tan et al., 2015). In this study, we selected the El Niño, neutral, and La Niña years based on data from sea surface temperature (SST) anomalies of the tropical Indian Ocean in the region + 0.5 °C and – 0.5 °C also known as the Niño 3.4 region. The gridded Extended Reconstructed Sea Surface Temperature version 4 (ERSSTv4) temperature data was used to study the ENSO events. We considered El Niño (La Niña) years as years with average SST anomalies above (below) temperature values of +0.5 °C (−0.5 °C) from October to March. The October to March period typically coincides with peak ENSO Conditions

Neutral years if the SST values are within - 0.5 °C < SST < 0.5 °C as shown in Fig. 14.

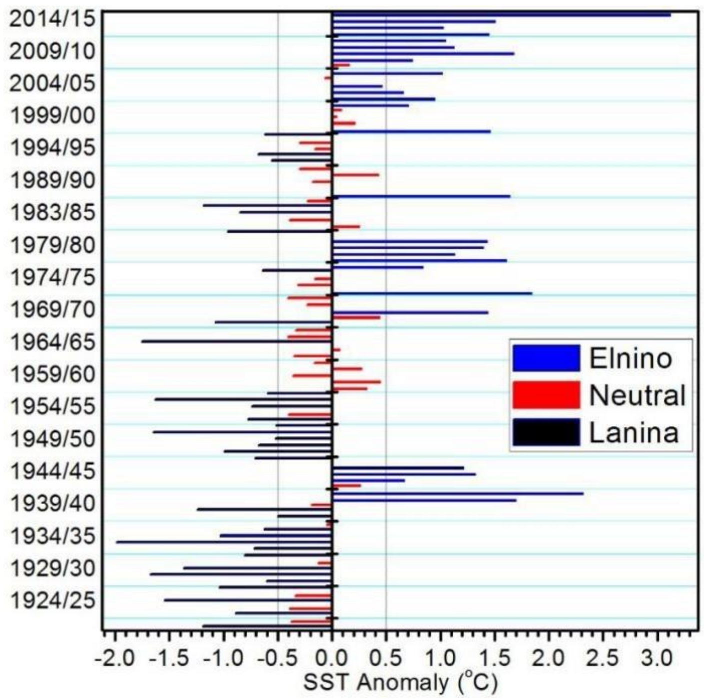

Fig. 14 Extended reconstructed sea surface temperature showing El Niño, neutral and La Niña years.

The SPI values in neutral, El Niño, and La Niña years were studied over East Africa from 1920 to 2015. The mean drought characteristics, magnitude, duration and even the dispersion, of drought magnitude in SPI-3, SPI-6 and SPI-12 are very similar in El Niño and La Niña events while the neutral years presented high dispersion in both drought magnitude and duration (Fig.15).

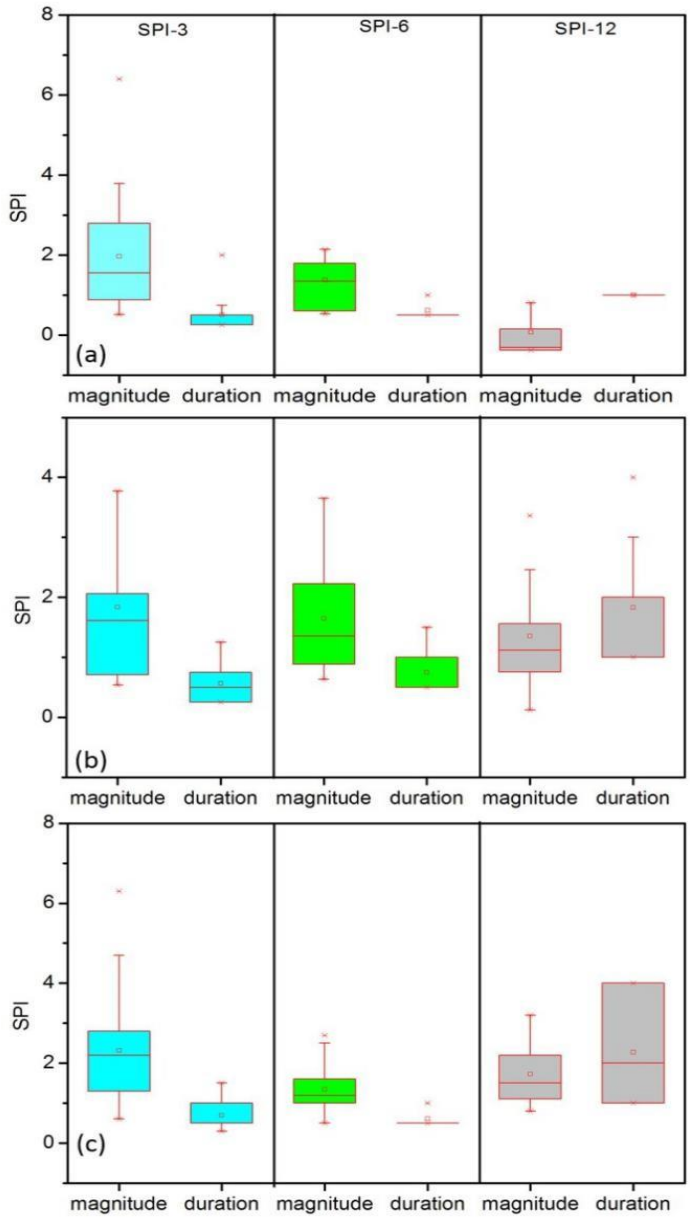

Fig. 15 Boxplots of mean magnitude and duration for (a) El Niño (b) neutral and (c) La Niña years

Results shown on Fig. 15a indicate that the mean drought duration during El Niño years were less than 1.5 years while the mean drought duration during neutral (La Niña) years was 3 (4) years (Figs. 15b and c).

In this study, there is no direct link between ENSO and drought over the East African region. But the association of drought in most El Niño and La Niña years suggests that the impact of

ENSO cannot be ruled out. Our results have supported reports that present teleconnections between drought and ENSO. Previous reports have shown that ENSO events normally peak during October to March periods which coincides with the short (SON) and long (MAM) rainy seasons of East Africa. This period coincides with the SON and MAM seasons and increased precipitation in East Africa. Considering the major drought episodes over the East Africa, our analysis has only agreed with the major droughts of 2011/12. Based on our results, 2011/12 was captured as an El Niño year with drought magnitudes captured by SPI-3 and SPI-6 as 2.8 and 0.5 respectively with drought duration of 3 and 6 months, respectively. The drought episode of 2011/12 affected countries like Somalia, Uganda, Kenya, Ethiopia, South-Sudan and other nearby countries.

3.6. Discussion

Generally, the actual precipitation expressed as a percentage deviation from normal (or long-term average) is the most commonly used drought indicator, although it has limited use/reliability for spatial comparison due to its dependence on the mean (Kumar et al., 2009). According to Solanki and Parekk (2014), the SPI represents a departure from the mean and is thus, expressed in standard deviation units as a normalized index in time and space. The departure from the mean is a probability indication of the severity of the wetness or drought that can be used for risk assessment. The application of data from 1920 in this study is considered most desirable as long records provide more reliable statistics for SPI, given that it is a statistical approach. As a result, SPI has gained importance in recent years as a potential drought indicator permitting comparisons across different precipitation zones (Kumar et al., 2009; Solanki and Parekk, 2014).

This study analyzed SPI values between 1920 and 2016 with actual precipitation and precipitation deviation from normal in East Africa, a generally low precipitation and drought prone region. The objective is to establish whether or not SPI can be used as a suitable indicator (when compared to conventionally adopted precipitation deviation-based approach for drought intensity assessment) over an extended region such as East Africa.

The results of the analysis show that very low or very high precipitation corresponded to very low or very high SPI values. Thus, SPI values adequately estimated the dryness or wetness when the precipitation is very low or very high, respectively. Table 2 shows that all periods that experienced dry spells (or drought) recorded low/negative anomaly and SPI values with the periods 1942-1943 recording the driest (-1.7) followed by 1983-1984 (-1.6). Similarly, the periods of wet spells reveal positive anomaly and SPI values with the wettest period being 2014-2015. The outcome of this study is in line with the SPI classes proposed by McKee et al. (1993). However, there is a marked variation between drought characteristics of magnitude, duration and intensity when viewed against temporal scales. In essence, no time scale recorded the highest in all 3 drought characteristics throughout the 95-year period of analysis (Table 3). This is similar to the observation of SPI at different time scales of 3, 6 and 12 months which reveal that for shorter time scales, there was a high temporal variability in dry and wet periods, whereas at longer time scales (12 months), frequency of dry and wet periods were considerably decreased (Fig. 5).

The results of this study indicate that drought characteristics analysis (magnitude, duration and intensity) using SPI can be adequately applied for drought intensity assessment particularly in regions such as East Africa where low precipitation and vulnerability to droughts is prevalent. The precipitation anomalies (Table 4), Mann-Kendall Trend and significance level of SPI-3, SPI-6 and SPI-12 (Table 5) and Mann-Kendall Trend and significance level of precipitation (Table 6) reveal varying results both temporally and spatially across the eight countries comprising the East African region covered in this study. For instance, the same drought level (SPI) may be prevalent in a country but the precipitation anomaly values may differ (Table 4). The drought of 1942-43 was worst hit in countries like Burundi, Rwanda, Ethiopia, Uganda and South-Sudan.

From 1983-84, Ethiopia, Kenya, Somalia, Uganda and South-Sudan experienced the worst drought episodes. Also, from 1991-92, Ethiopia, Kenya, and Somalia experienced worst drought spells, while in 1996-97, the highest effect was observed in Ethiopia. Table 5 reveals that out of eight countries, SPI-12 detects significant positive (insignificant positive) trend over 3(2) countries and insignificant negative trends over 3 countries. SPI-6 detects insignificant positive trend over 6 countries and insignificant negative trend over 2 countries. SPI-3 detects insignificant positive trends over 5 countries while insignificant negative trends in 3 stations. At regional (continental scale), there was no significant trend in SPI-3, SPI-6 or SPI-12. The results in Table 6 show that most countries experience oscillations between wet and dry conditions while few countries are getting wetter with few others getting more arid. At regional (continental scale), there was no significant trend in precipitation. There was no significant change in precipitation in annual rainy seasons during the study period. As no annual trend was observed in the precipitation amount, we applied SPI to study precipitation address potential changes in precipitation extremes.

There is expected to be some time lag due to the unique vegetation types which, according to Abbas et al. (2014), should have different capacity of water storage. The humid area covering most of Uganda as shown on Fig. 1 (with predominantly tall and dense forests) are expected to have a longest time lag because, according to Allen (2008), forests possess the best capacity of water retention with deeper roots to tap groundwater. Conversely, arid and semi-arid areas such as Kenya, Somalia and Ethiopia are covered mostly by grasses and should have shorter time lag due to the lower capacity of water retention for grasses. South-Sudan and a significant area of Tanzania are sub-humid areas largely covered by crops. Generally, the water storage capacity of crops is likely similar to or even lower than that of grasses, and Grünzweig et al. (2015) posits that artificial irrigation could alter the time lag for regions engaged in irrigation agriculture. It is therefore, expected that semi-arid areas should have a time lag similar to or longer than arid areas (Cong et al., 2017). This pattern is largely similar to the outcome of the study as shown on Tables 4, 5 and 6, and Figs 4, 8 and 9.

4. Conclusions

In this study, the SPI approach applied to this study adequately explained the drought conditions across the East African region between 1920 and 2015. The drought characteristics of magnitude, duration and intensity collectively explained the severity levels of drought within the study area. It is expected that the outcome of this study could be applied elsewhere in sub-Saharan Africa where precipitation is limited and likelihood of drought is high.

The result from the 96 years (from 1920 to 2015) data records shows that there are a total of 41 wet years and 46 drought years. The anomaly of the wet years and dry years were obtained when precipitation was above and below normal conditions respectively. The years 1961, 1967, 1997, 2007 and 2015, were adjudged the wettest while 1943, 1983, 1993, 1997 and 2003 were adjudged the driest. Both the positive and negative peak of SPI coincided with the positive and negative anomaly peaks, respectively. The computed SPI at different time scales of 3, 6 and 12 months indicated that for shorter time scales, there was high temporal variability in dry and wet periods, whereas at longer time scales (12 months), frequency of dry and wet periods were considerably decreased.

Years with high drought magnitude ranged from 1920-22, 1926-29, 1942-46 and 1947-51 with SPI values corresponding to 2.2, 3.2, 3.4 and 2.6, respectively while years with low drought magnitude ranged from 1930-31, 1988-89 and 2001-02 with values as 0.2, 0.12 and 0.15, respectively. The longest droughts occurred from 1929-29, 1937-41, 1942-46, 1947-51, 1952-56, and 1958-61 with values in years as 3, 4, 4, 4, 4, and 3 years, respectively, while the shortest droughts occurred in time period of 1 year and ranged from 1930-31, 1964-65, 1979-80, 1981-82, 1983-84, 1988-89, 1991-92, 1993-94, 1996-97 and 2001-02.

Our study also indicated that high values of SPI slope are clustered at higher latitudes from 0 to 12^{o} while low trend values are clustered between -2 and 2^{o} south of the study region which is an indication that drought is prevalence in the northern section than southern section of the study area. Both high and low slope values of SPI are clustered at lower latitudes between 0 to 1500 meters, and at the foot hills of mountains. The SPI trends showed high positive (negative) pixels above (below) the zero-trend mark, indicating that drought prevails in both low and high elevation areas up to 2000 m.

In terms of ENSO impacts on drought over the region, the mean characteristics, magnitude, duration and even the dispersion, of drought magnitude in SPI-3, SPI-6 and SPI-12 are very similar in El Niño and La Niña years while the neutral years presented high dispersion in both drought magnitude and duration. The mean drought duration during El Niño years were less than 1.5 years while the mean drought duration during neutral (La Niña) years was 3 (4) years which suggest that there is no direct link between ENSO and drought over the East African region. But the association of drought in most El Niño and La Niña years suggests that the impact of ENSO cannot be ruled out since peak ENSO events occur during October to March periods which coincides with the short (SON) and long (MAM) rainy seasons of East Africa.

Furthermore, the outcome of this study indicates that SPI can be reliably suitable and most applicable in drought studies within the study area as it provides for analysis in multi-temporal levels such as monthly, single seasonal, multi-seasonal, and annual droughts, thereby allowing for a spatio-temporal scale of analysis that creates the room for SPI to provide accurate meteorological and agricultural drought analysis. To this extent, the study provides policy makers the necessary information that is critical to local adaptation, increased resilience and mitigation measures in the face of a vulnerable eco-climatic system triggered by a continuously changing climate within East Africa as well as other parts of sub-Saharan Africa.

Our study is particularly relevant in its ability to depict continuous and synoptic drought conditions all over East Africa, providing vital information to farmers and policy makers, using very cost-effective method. This is particularly the case in view of the assertion by Karavitis et al. (2011) that "effective (and reliable) information and early warning systems based on indicators such as the SPI are the foundation for overall effective drought adaptation (and resilience) plans".

Finally, the adoption of SPI for this study demonstrates the fact that it is a robust concept, unambiguous in calculation and understanding, temporally flexible, spatially meaningful, and widely applicable, a basis for which it is considered a powerful tool for drought studies as clearly amplified by Cheval (2015).

Acknowledgements

This work was jointly supported by the CAS Strategic Priority Research Program (No. XDA19030402), the National Key Research and Development Program of China (no. 2016YFD0300101), and "Taishan Scholar" Project of Shandong Province (No. TXXD 201712). The authors would like to show great appreciations to the anonymous reviewers and the editor for their valuable comments and suggestions.

References

Abbas, S., Nichol, J.E., Qamer, F.M., Xu, J. (2014). Characterization of drought development through remote sensing: A case study in central Yunnan, China. Remote Sens. 6(6): 4998–5018.

Abbink, J., K. Askew, D.F. Dori, E. Fratkin, E.C. Gabbert, J. Galaty, S. LaTosky, J. Lydall, et al., (2014). Lands of the Future: transforming pastoral lands and livelihoods in eastern Africa. Working Paper No. 154, Max Planck Institute for Social Anthropology.

Allen, C.D. (2008). Mechanisms of plant survival and mortality during drought: why do some plants survive while others succumb to drought? New Phytol. 178 (4), 719.

American Meteorological Society (1997). Meteorological drought-policy statement. Bull Am Meteorol Soc 78:847–849

Bates, B.C., Kundzewicz, Z.W., Wu, S.and Palutikof, J.P. (eds.). (2008). Climate Change and Water. Technical Paper of the Intergovernmental Panel on Climate Change, IPCC Secretariat, Geneva. Available from https://www.ipcc.ch/pdf/technical-papers/climate-change-water-en.pdf - 28/doc13.pdf (accessed: June, 2018).

Cong, D., S. Zhao, C. Chen and Z. Duan (2017). Characterization of droughts during 2001–2014 based on remote sensing: A case study of Northeast China. Ecological Informatics 39: 56–67

Dai, A., Lamb, P., Trenberth, K.E., Hulme, M., Jones, P.D. and Xie, P. (2004) The Recent Sahara Drought is Real. International Journal of Climatology 24: 1323-1331

Eze, J.N. (2018) Drought occurrences and its implications on the households in Yobe state, Nigeria. Geoenvironmental Disasters 5:18, 1-10

Funk, C., Dettinger, M. D., Michaelsen, J. C., Verdin, J. P., Brown, M. E., Barlow, M., & Hoell, A. (2008). Warming of the Indian Ocean threatens eastern and southern African food security but could be mitigated by agricultural development. Proceedings of the National Academy of Sciences, 105(32), 11081-11086.

Funk, C., Hoell, A., Shukla, S., Bladé, I., Liebmann, B., Roberts, J. B., Robertson, F. R., and Husak, G. (2014) Predicting East African spring droughts using Pacific and Indian Ocean sea surface temperature indices, Hydrol. Earth Syst. Sci., 18, 4965–4978, https://doi.org/10.5194/hess-18-4965-2014.

Funk, C., Husak, G., Michaelsen, J., Shukla, S., Hoell, A., Lyon, B., et al. (2013). Attribution of 2012 and 2003-12 rainfall deficits in eastern Kenya and southern Somalia. In Explaining extreme events of 2012 from a climate perspective. Bulletin of the American Meteorological Society. 94, S45-S48.

Funk, C., Peterson, P., Landsfeld, M., Pedreros, D., Verdin, J., Shukla, S., Husak, G., Rowland, J., Harrison, L., Hoell, A., and Michaelsen, J. (2015) The climate hazards infrared precipitation with stations-a new environmental record for monitoring extremes, Sci. Data, 2, 150066, https://doi.org/10.1038/sdata.2015.66

Ghulam A, Qin Q, Zhan Z (2007a) Designing of the perpendicular drought index. Environ Geol 52(6):1045–1052

Ghulam A, Qin Q, Teyip T, Li Z-L (2007b) Modified perpendicular drought index (MPDI): a real-m time drought monitoring method. ISPRS J Photogramm Remote Sens 62:150–164

Gibbs W., Maher J. (1967) Rainfall deciles as drought indicators. Australian Bureau of Meteorology Bulletin, Melbourne: 48

Grünzweig, J.M., Valentine, D.W., Chapin III, F.S. (2015). Successional changes in carbon stocks after logging and deforestation for agriculture in Interior Alaska: implications for boreal climate feedbacks. Ecosystems 18 (1), 132–145

Hao, C., Zhang, J., Yao, F. (2015). Combination of multi-sensor remote sensing data for drought monitoring over Southwest China. J. Appl. Earth Obs. Geoinf. Int. https://doi.org/10.1016/j.jag.2014.09.011.

Harvest Choice (2015). "AEZ tropical (5-class, 2009)." International Food Policy Research Institute, Washington, DC., and University of Minnesota, St. Paul, MN. Available online at http://harvestchoice.org/data/aez5_clas

Haroon, M.A., Zhang, J. and Yao, F. (2016). Drought monitoring and performance evaluation of MODIS-based drought severity index (DSI) over Pakistan. Natural Hazards 84(2): 1349-1366

Huete, A. (1988) A soil-adjusted vegetatio n index (SAVI). Remote Sens Environ 25:295–309

Igbawua, T., Zhang, J., Yao, F., Zhang, D. (2018). Assessment of moisture budget over West Africa using MERRA-2's aerological model and satellite data. Climate Dynamics https://doi.org/10.1007/s00382-018-4126-2

Kalisa, W., Igbawua, T., Henchiri, M., Ali, S., Zhang, S., Bai, Y., Zhang, T. (2019) Assessment of climate impact on vegetation dynamics over East Africa from 1982 to 2015. Scientific Reports, | 9:16865 | https://doi.org/10.1038/s41598-019-53150-0

Karavitis, C.A., S. Alexandris, D.E. Tsesmelis and G. Athanasopoulos (2011). Application of the Standardized Precipitation Index (SPI) in Greece. Water, 3: 787-805; doi:10.3390/w3030787

Kim, T., Yoo, C., Valdes, J.B. (2003) Non parametric Approach for estimating effects of ENSO on return periods of Drought, Water Engineering, 7(5), 629-636.

Kogan, F.N. (1995) Application of vegetation index and brightness temperature for drought detection. Adv Space Res 15:91–100

Kogan, F.N. (2001) Operational space technology for global vegetation assessment. Bull Am Meteorol Soc 82:1949–1964

Kogan, F.N., Gitelson, A., Zakarin, E., Spivak, L., Lebed L (2003) AVHRR-based spectral vegetation index for quantitative assessment of vegetation state and productivity: calibration and validation. Photogramm Eng Remote Sens 69:899–906

Kumar, M.N., C.S. Murthy, M.V.R. Sesha-Saib and P.S. Roy (2009). On the use of Standardized Precipitation Index (SPI) for drought intensity assessment Wiley Inter Science Meteorol. Appl. 16: 381–389

Lambin, E., Ehrlich, D. (1995) Combining vegetation indices and surface temperature for land-cover mapping at broad spatial scales. Int J Remote Sens 16:573–579

Lei, T., Pang, Z., Wang, X., Li, L., Fu, J., Kan, G., et al. (2016). Drought and carbon cycling of grassland ecosystems under global change: a review. Water 8(10), 460.

Liu, H.Q., Huete, A. (1995) A feedback based modification of the NDVI to minimize canopy background and atmospheric noise. IEEE Trans Geosci Remote Sens 33:457–465

Liu, Q., Zhang, S., Zhang, H., Bai, Y., Zhang, J. (2019) Monitoring drought using drought indices based on remote sensing. Science of the Total Environment 711 (2020) composite

134585.

Love, R. (2009) Economic Drivers of Conflict and Cooperation in the Horn of Africa, Chatham House Briefing Paper, December, available at: www.chathamhouse.org/ publications/papers /view/109208 (last access: 18 April 2012).

Masih, I., Maskey, S., Mussá, F.E.F. a0nd Trambauer, P. (2014) A review of droughts on the African continent: a geospatial and long-term perspective, Hydrol. Earth Syst. Sci., 18, 3635–3649, https://doi.org/10.5194/hess-18-3635-2014

McKee, T.B., Doesken, N.J. and Kleist, J. (1993) The relationship of drought frequency and duration to time scales. *In*: Eighth conference on applied climatology. American Meteorology Society, Anaheim, CA, 179–184

McQuigg, J. (1954). A simple index of drought conditions. Weather Wise 7:64–67

Morton, J. and Kerven, C. (2013). Livelihoods and basic service support in the drylands of the Horn of Africa. Brief prepared by a Technical Consortium hosted by CGIAR in partnership with the FAO Investment Centre. Technical Consortium Brief 3. Nairobi: International Livestock Research Institute.

Mu, Q., Zhao, M., Kimball, J.S., McDowell, N.G., Running, S.W. (2013). A remotely sensed global terrestrial drought severity index. Bull Am Meteorol Soc 94:83–98

Munger, T.T. (1916). Graphic method of representing and comparing drought intensities. Monthly Weather Rev 44:642–643

Niemeyer, S. (2008). New drought indices. Options Mditerranennes Sri A Sminaires Mditerranens

80:267–274

O'Connor, T.G. (1995). Transformation of a savanna grassland by drought and grazing. African Journal of Range and Forage Science. 12 (2): 53–60.

Palmer, W.C. (1968). Keeping track of crop moisture conditions, nationwide: the new crop moisture index. Weather Wise 21: 156–161

Pramudya, Y. and T. Onishi (2018). Assessment of the Standardized Precipitation Index (SPI) in Tegal City, Central Java, Indonesia. IOP Conf. Series: Earth and Environmental Science 129: 1-9

Sandholt, I., Rasmussen, K., Andersen, J. (2002). A simple interpretation of the surface temperature/vegetation index space for assessment of surface moisture status. Remote Sens Environ 79:213–224

Schubert, S.D., Stewart, R.E.,Wang, H., Barlow,M., Berbery, E.H., Cai,W., et al., (2016). Global meteorological drought: a synthesis of current understanding with a focus on SST drivers of precipitation deficits. J. Clim. 29 (11), 3989–4019.

Solanki, J.K. and F, Parekh (2014) Drought Assessment Using Standardized Precipitation Index International Journal of Science and Research, 3(7): 1073-1076

Svoboda, M.D., LeComte, D., Hayes, M.J. (2002). The drought monitor. Bull Am Meteorol Soc 93:1181–1190

Tan, C., Yang, J., Li, M., 2015 Temporal-Spatial Variation of Drought Indicated by SPI and SPEI in Ningxia Hui Autonomous Region, China, Atmosphere, 6, 1399-1421;

doi:10.3390/atmos6101399

Tarhule, A., Woo, M.-K. (1997). Towards an interpretation of historical droughts in northern Nigeria. Climatic Change 37: 601–616

Um, M., Y. Kim, D. Park, and J. Kim. (2017). Effects of different reference periods on drought index estimations from 1901 to 2014. Hydrology and Earth System Sciences 21: 4989–5007

von Grebmer, K., Bernstein, J., Nabarro, D., Prasai, N., Amin, S., Yohannes, Y., Sonntag, A., Patterson, F., Towey, O., Thompson, J. (2016). Global Hunger Index: Getting to Zero Hunger. Welthungerhilfe, International Food Policy Research Institute, and Concern Worldwide, Bonn, Washington, DC, and Dublin

Waggoner, M.L. and O'Connell, T.J. (1956). Antecedent precipitation index. Weekly Weather Crop Bull XLIII: 6–7

Weghorst, K. (1996) The reclamation drought index: guidelines and practical applications. Bureau of Reclamation, Denver

Yang, H. and Huntingford, C. (2018). Drought likelihood for East Africa. Nat. Hazards Earth Syst. Sci., 18: 491–497

Yao, N., Y. Li., T. Lei. and L. Peng. (2018). Drought evolution, severity and trends in mainland China over 1961–2013. Science of the Total Environment 616–617: 73–89

Yao, Y., Liang, S., Qin, Q., Wang, K. (2010). Monitoring drought over the conterminous United States using MODIS and NCEP Reanalysis-2 data. J. Appl. Meteorol. Climatol. 49: 1665–1680

Highlights

1. Assessment of drought exceedance and return years over East Africa from 1920 to 2016.

2. Probability of drought occurrence is high when severity is low and such droughts occur at short time intervals and not all severest drought took longer periods.

3. ENSO impacts on East Africa’s drought in most El Niño and La Niña years.

4. Drought prevails in both low and high elevation areas up to 2000 m over study area.

5. Drought magnitude, frequency, exceedance probability and return years assessed by Joint Probability Density Function (JPDF).

Spatio-Temporal analysis of drought and return periods over the East African region using Standardized Precipitation Index from 1920 to 2016

Wilson Kalisa[1,2], Jiahua Zhang[2,3*], Tertsea Igbawua[4], Fanan Ujoh[5], Obas John Ebohon[5], Jean Nepomuscene Namugize[6], Fengmei Yao[7]

1. Agricultural Climate Change Mitigation, College of Automation and Electrical Engineering, Qingdao University, Qingdao, 266071, China

2. Remote Sensing and Digital Earth Center, College of Computer Science and Technology, Qingdao University, Qingdao, 266071, China

3. Key Laboratory of Digital Earth Science, Aerospace Information Research Institute, Chinese Academy of Sciences, Beijing, 100094, China

4. Department of Physics, Federal University of Agriculture, Makurdi, Nigeria

5. Center for Sustainability and Resilient Infrastructure and Communities (SaRIC), School of the Built Environment and Architecture, London South Bank University, London, UK

6. Rwanda Polytechnic, Integrated Polytechnic Regional Center, College of Kigali, Rwanda

7. Key Laboratory of Computational Geodynamics, University of Chinese Academy of Sciences, Beijing, 100049, China

*Corresponding- author: Prof. Jiahua Zhang, email address: zhangjh@radi.ac.cn

Revised to “*Agriculture Water Management*”

Abstract East African region is susceptible to drought due to high variation in monthly precipitation. Studying drought at regional scale is vital since droughts are considered a ‘creeping’ disaster by nature with devasting and extended impact often requiring long periods to reverse the recorded damages. This study assessed drought exceedance and return years over East Africa from 1920 to 2016 using Climate Research Unit (CRU) precipitation data records. Meteorological drought, where precipitation is the central quantity of interest, was adopted in the work. Standardize Precipitation Index (SPI) was used to study long term meteorological droughts and also to assess drought magnitude, frequency, exceedance probability and return years using Joint Probability Density Function (JPDF). Also, Mann-Kendall trend analysis was applied to precipitation and SPI to investigate the trend changes. Results showed that years with high drought magnitude ranged from 1920-22, 1926-29, 1942-46 and 1947-51 with values corresponding to 2.2, 3.2, 3.4 and 2.6, respectively while years with low drought magnitude ranged from 1930-31, 1988 89 and 2001-02 with values as 0.2, 0.12 and 0.15, respectively. The longest droughts occurred from 1926-29, 1937-41, 1942-46, 1947-51, 1952-56, and 1958-61 with values in years as 3, 4, 4, 4, 4, and 3 years, respectively, while the shortest droughts occurred in time period of 1 year and ranged from 1930-31, 1964-65, 1979-80, 1981-82, 1983-84, 1988-89, 1991-92, 1993-94, 1996-97 and 2001-02. Also, it was demonstrated that probability of drought occurrence is high when severity is low and such droughts occur at short time intervals and not all severest drought took longer periods. The SPI trends indicate high positive (negative) pixels above (below) the zero trend mark, indicating that drought prevails in both low and high elevation areas up to 2000 m. There was no direct link between ENSO and drought but arguably the association of drought in most El Niño and La Niña years suggests that the impact of ENSO cannot be ruled out since peak ENSO events occur during October to March periods which coincides with the short (SON) and long (MAM) rainy seasons of East Africa. The study is particularly relevant in being able to depict continuous and synoptic drought condition all over East Africa, providing vital information to farmers and policy makers, using very cost-effective method.

Keywords Meteorological Drought, Joint Probability Density Function (JPDF), SPI, ENSO, Drought Risk Mapping.

Introduction

Several studies indicate that droughts are among the most destructive natural disasters, negatively impacting livelihoods including crops and livestock, as well as other natural resources such as water, ecology, and biodiversity (Haroon et al., 2016; Lei et al., 2016; Schubert et al., 2016; Igbawua et al., 2018; Yao et al., 2018; Liu et al., 2020). The American Meteorological Society (1997) categorizes droughts into meteorological, agricultural and hydrological mainly on the basis of duration, impact and recovery rate. According to Ghulam et al. (2007) and Haroon et al. (2016), meteorological drought refers to a sustained period of three months or more during which monthly precipitation remains well below the long-term average. Agricultural drought occurs when there is an imbalance between water availability and demand in a farmland ecosystem, where water demand by plants is more as compared to supply. Hydrological droughts occur when deficiencies in surface and subsurface water supplies become evident in terms of reduced stream flow and reduction in ground water. For the purpose of this study however, the assumption is that "drought occurs when precipitation deficit exceeds some critical level beyond which the prevailing adaptive mechanisms fail to cope", as defined by Tarhule and Woo (1997). The occurrence of drought has been recorded across all continents and under all climatic regions with low and high mean precipitation (Um et al., 2017) with varying degree, intensity, impact and duration.

In recent decades, the occurrence and incidence of drought has been aggravated with the increase in global climate change (IPCC, 2014). For Africa, O'Connor (1995) reported that remotely sensed data analysis from National Aeronautics and Space Administration (NASA) reveal that about 900,000 km^2 of previous savanna grassland in the African region had been severely degraded between the early 1960s and 1986 due to persistent occurrences of drought, while Bates et al., (2008) estimated that one-third of African population live in drought-prone areas. Yang & Huntingford (2018) revealed historical precipitation estimated by Climate Hazards Group InfraRed Precipitation with Station data (CHIRPS) (Funk et al., 2015) shows that during

August, September and October (ASO) of 2016, most of East Africa (particularly Somalia, Ethiopia and Kenya) had a reduction of 40% or more in precipitation compared to a baseline ASO period 1981–2015. Several studies confirm that the East African region ranks among the most vulnerable drought-prone regions of the world with a high potential for increased risk of drought related water and food shortages as recorded in as recent as year 2016/2017 (Love, 2009; Masih et al., 2014; Funk et al., 2014, 2015; Yang and Huntingford, 2018). The threat of drought is expected to further aggravate the existing widespread poverty and food insecurity (Funk et al., 2008, 2013, 2015; von Grebmer et al., 2016). The situation is similar within other regions of subsaharan Africa. In West Africa, Dai et al. (2004) reported that there is about 40% decline in annual precipitation total from the year 1968–1990 as compared with the 30 years between 1931 and 1960. Thus, frequent drought occurrences within the West African region have caused famine and are threatening the human existence in African savanna regions and consequently making the households highly vulnerable to drought (Eze, 2018).

Droughts are considered a ‘creeping’ disaster by nature with devasting and extended impact often requiring long periods to reverse the recorded damages. It is therefore crucial that consistent drought monitoring is carried out to provide decisive policy support for long- and medium-term planning of mitigative measures. Typically, at the turn of the 20th century, scientific studies had adopted climatic (temperature and precipitation) and hydrological (soil moisture and stream flow) indicators as main input towards the generation of indices for quantitative modelling of drought severity (Kincer, 1919; Munger, 1916; McQuigg, 1954; Waggoner and O’Connell, 1956). However, further advances in the study of drought (beginning from the latter part of the 20th century into the 21st century) led to the identification of over 150 indices used for drought studies (Niemeyer, 2008) across various regions with different climatic conditions. The most prominently adopted contemporary indices for drought research include, but not limited to: decile index (DI) by Gibbs and Maher (1967); Palmer drought severity index (PDSI) by Palmer (1968), standardized precipitation index (SPI) applied by McKee et al. (1993); reclamation drought index (RDI) by Weghorst (1996); US Drought Monitor (USDM) applied by Svoboda et al. (2002); optimized meteorological and vegetation drought indices (OMDI and OVDI) proposed by Hao et al. (2015); composite drought indices using multivariable linear regression (MCDIs) developed by Liu et al. (2020).

Recent drought studies have relied on the availability of data from different remote sensing platforms due largely to the synoptic coverage it provides for analysis over a wide region.

Numerous methods have been developed for the application of remotely sensed data in drought studies. These include normalized difference vegetation index (NDVI) based conceptualization such as vegetation condition index (VCI) (Kogan 1995), enhanced vegetation index (EVI) (Liu and Huete 1995), soil adjusted vegetation index (SAVI) (Huete 1988), temperature vegetation index (TVX) (Lambin and Ehrlich, 1995), Deviations from NDVI (Anyamba et al., 2001), vegetation health index (VHI) (Kogan, 2001), temperature condition index (TCI) (Kogan, 1995; Kogan et al., 2003), and temperature vegetation dryness index (TVDI) (Sandholt et al., 2002).

More advanced methods now include satellite derived indices such as perpendicular drought index (PDI) (Ghulam et al., 2007a); modified perpendicular drought index (MPDI) (Ghulam et al., 2007b); effective drought index (EDI) (Yao et al., 2010); and Drought severity index (DSI) proposed by Mu et al. (2013) and applied by Haroon et al. (2016).

For the purpose of this study, the SPI proposed by McKee et al. (1993), and applied in Indonesia by Pramudya and Onishi (2018) will be adopted for the analysis of drought across the East African region. The SPI is considered most applicable for this study because it provides for drought analysis in multi-temporal levels such as monthly, single seasonal, multi-seasonal, and annual basis. This level of spatio-temporal scale analysis allows for the SPI to provide accurate meteorological and agricultural drought analysis.

2.0 Methodology

2.1 Study Area

The study area covers eight countries consisting of Ethiopia, Kenya, Rwanda, Uganda, Tanzania, Burundi, Somalia and South-Sudan (Fig. 1). The climate of the region is influenced by a number of factors ranging from combination of the high altitude and the westerly monsoon winds that originate from the Ethiopian Highlands and Rwenzori Mountains. Generally, majority of the region's countries experience two distinct precipitation regimes: "long rains" which extend during March–May (MAM), and a season with "short rains", which lasts from October to December (OND). Figure 1 shows that much of Uganda and Somalia are humid and arid, respectively while much of Ethiopia is semi-arid and arid. South-Sudan and Tanzania are largely sub-humid, with Kenya containing a vast area of aridity. Rwanda and Burundi are largely tropical highlands.

The major livelihood sources include pastoralism and agro-pastoralism, rangeland cultivation, small-holder agriculture, milk production and dairy products processing (Morton and Kerven, 2013; Abbink et al., 2014).

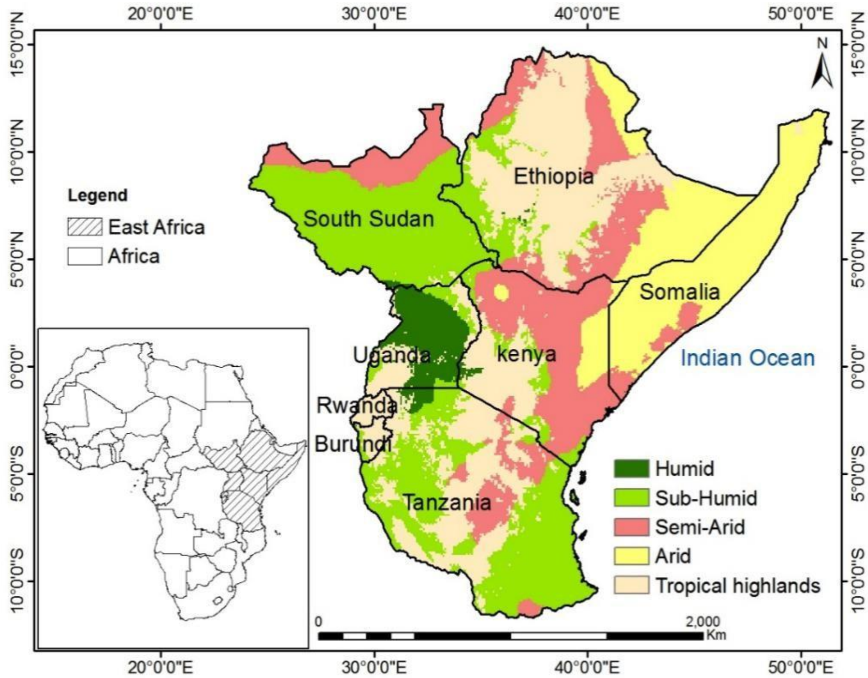

Fig. 1 Study area (Harvest Choice, 2015)

2.2 Data sets and methods

The precipitation data set used in this work is the Climate Research Unit (CRU) data developed by University of East Anglia. The data was retrieved from http://data.ceda.ac.uk/badc/cru/data/cru_ts/cru_ts_4.00/data/ at a spatial resolution of 0.5 x 0.5 degrees covering a temporal range of 1920 to 2015. The Standardized Precipitation Index (SPI) developed by McKee et al. (1993) is a popular index that is used to characterize drought at different time scales. SPI is computed by fitting a gamma distribution function to precipitation data of given frequency distribution over an area, and subsequently transforming the gamma distribution to a normal distribution with a mean and variance of zero (0) and one (1) respectively (Suryabhagavan, 2016). The aim of doing this is to minimize skewness in the data to zero. The Gamma distribution is widely used to represent precipitation time series (Guttman, 1999). The drought magnitude was obtained as the cumulative SPI over the drought months taken as a positive value. The intensity (drought severity) was computed as the magnitude divided by drought duration. The general technique for detecting changes in precipitation and drought is trend analysis. In this work, Trend analysis of precipitation and SPI will reveal will reveal the trends in drought over East Africa. Since, the input parameter for SPI computation is precipitation, trend analysis of precipitation will be done in order to study the local changes in climate. The Mann-Kendall non-parametric test was adopted in this work to assess the trends in precipitation and SPI and, also test the statistical distribution of the data records. Mann-Kendall was most preferred because it works well to avoid the problem caused by skewness of which precipitation is a kind of data that may be either negatively or positively skewed due to the existence of extreme values (Mahajan & Dodamani, 2015).

2.2.1 SPI

In calculating SPI, we adopt methods by Haroon, et al. (2016) and Guttman (1999), and fit a

→

probability distribution to long-term monthly precipitation records. The mean $(\vec{x})$, standard deviation (s) and skew (sk) are determined as follows:

mean $(\vec{x}) = \frac{\sum X}{N}$ (1)

standard deviation (s) = $\sqrt{\frac{\sum(X-\vec{X})^2}{N}}$ (2)

skewness (sk) = $\frac{N}{(N-1)(N-2)} \cdot \frac{\sum(X-\vec{X})^2}{N}$ (3)

where, x is the precipitation time series and N is the length of data records. The precipitation data are transformed by the log normal (ln) and the mean of those values is computed. The transformed values are further subjected to the constant U, which is used to compute the shape and Scale parameter as follows:

Log mean $= \vec{X}_h = \frac{\ln(X)}{N}$ (4)

$U = \ln(X) - \frac{\ln(X)}{N}$ (5)

Shape $(\beta) = \frac{1}{4U}[1+\sqrt{\frac{4U}{3}}$ (6)

and, Scale $(\alpha) = \frac{\vec{X}}{\beta}$ (7)

Further, the log values are transformed by the gamma distribution, incorporating the shape and scale values:

Cumulative Gamma function G(x) = $\frac{1}{\alpha^{\beta}\Gamma\beta}\int_{o}^{x} x^{\beta-1} e^{-\frac{x}{\alpha}} dx$ (8)

Similarly, $t = \sqrt{\ln\left(\frac{1}{(1-X_g)^2}\right)}$, where $0.5 < X_g \leq 1.0$

and, we perform T transform as $t = \sqrt{\ln\left(\frac{1}{X_g^2}\right)}$, where $0 < X_g \leq 0.5$ (9)

and the SPI= $-t + \frac{C_0 + C_1 t + C_2 t^2}{1 + d_1 t + d_2 t^2 + d_3 t^3}$ where $0 < X_g \leq 0.5$ (10)

or SPI= $t - \frac{C_0 + C_1 t + C_2 t^2}{1 + d_1 t + d_2 t^2 + d_3 t^3}$ where $0.5 < X_g \leq 1.0$ (11)

The constants expressed in equations (10) and (11) are given as follows

C_0=2.515517,	d_1= 1.432788
C_1=0.802853,	d_2= 0.189269
$C_2 = 0.010328$,	$d_3 = 0.001308$

2.2.2 Drought Magnitude, Duration and Intensity

The drought magnitude (D_M) was obtained as follows

$$D_M = -\sum_{i=1}^{n} SPI_{ij} \quad (12)$$

where D_M is the drought magnitude, n is the number of months with drought event at j timescale. Drought intensity (D_I) is the ratio of drought magnitude (D_M) to drought duration (D_d) as follows:

$$D_I = \frac{D_M}{D_d} \quad (13)$$

2.2.3 Mann-Kendall Trend Test

The Mann-Kendall trend test is given as

$$S = \sum_{i=1}^{n-1} \sum_{j=i+1}^{n} sgn(x_j - x_i) \qquad (14)$$

where is the time series ranked from x_i i= 1, 2,………n-1 and x_j from j=i+1,2,……..n. All the data values are taken as reference point to which comparison is done with the rest of the data values x_j such;

$$sgn(x_j - x_i) = \begin{cases} +1, > (x_j - x_i) \\ 0, = (x_j - x_i) \\ -1, < (x_j - x_i) \end{cases} \qquad (15)$$

The statistics of variance is given as

$$Var(S) = \frac{n(n-1)(2n+5) - \sum_{i=1}^{m} t_i(i)(i-1)(2i+5)}{18} \qquad (16)$$

where is the number of ties up to sample value t_i i. Z_c is the test statistics and is calculated as $Z_c =$

$$\begin{cases} \frac{S-1}{\sqrt{Var(S)}}, S > 0 \\ 0, S = 0 \\ \frac{S-1}{\sqrt{Var(S)}}, S < 0 \end{cases} \qquad (17)$$

Z_c describes a Standard Normal Distribution (SND) and positive and negative values of Z_c shows an upward and downward trend respectively. According to Mondal et al. (2012), a significance level γ is also used in testing either an upward or downward monotone trend, if Z_c is greater than $Z_{\gamma/2}$ then the trend is considered significant and vice versa.

2.2.4 Sen's Trend Estimator

The Sen's trend estimator test was described by Sen (1968) and the magnitude of the trend is given by

$$T_i = \frac{x_j - x_k}{j - k} \qquad (18)$$

where x_j and x_k are considered as data points j and k (j>k) compatibly. The median of these N values of T_i is represented as Sen's estimator of slope which is given as

$$Q_i = \begin{cases} T_{\frac{N+1}{2}} & N \text{ is odd} \\ \frac{1}{2}\left(T_{\frac{N}{2}} + T_{\frac{N+2}{2}}\right) & N \text{ is even} \end{cases} \qquad (19)$$

Positive and negative values of Q_i represent upward (increasing) and downward (decreasing) trends, respectively.

In order to assess the spatio-temporal occurrence of drought over East Africa, the 3-month, 6-month and 12-month SPI was used to study drought in the long term. This period is enough for drought frequency and intensity assessment. The SPI was computed on monthly scale so that the consistency of drought duration and intensity can be determined according to Table 1.

Table 1 Standard SPI table (McKee et al., 1993)

SPI value	Description
2 >	Extremely wet

1.5 – 1.99	Very wet
1.0 – 1.49	Moderately wet
0 – 1.0	Mildly wet
-1.0 – 0	Mildly drought
-1.5 – -1.0	Moderately drought
-2.0 – -1.5	Severe drought
-2 <	Extreme drought

From a statistical point of view, droughts are considered as multivariate events whose dimension and treatment depends on their characteristics such as the duration, severity and frequency (Gonzalez et al., 2004). Most studies have proposed the Joint Probability Distribution Function (JPDF) for determining probabilistic characteristic because drought severity and duration are often difficult to treat separately.

Given a set of observations y_i........y_n, a mathematical expression of bivariate Kernel probability density estimator f_{SD} is given as (kim et al., 2003):

$$f_{SD}(s,d) = \frac{1}{n h_s h_d}\sum_{i=1}^{n}\left\{K\left(\frac{S-S_i}{h_s}\right)K\left(\frac{d-d_i}{h_d}\right)\right\} \qquad (20)$$

The joint return period of drought (T_{Sd}) is given as (kim et al., 2003):

$$T_{Sd} = \frac{N}{n[1 - f_{SD}(s,d)]} \qquad (21)$$

where N is the numbers of years.

3. Results

3.1. Seasonal Characteristics of Precipitation and Precipitation Anomaly over East Africa from 1920 to 2015

The seasonal characterization of precipitation over the East African region (Fig. 2) reveals that long precipitations occur during the period of March to May (MAM) while short precipitations occur from the period of October to December (OND). The study analysis revealed that peak annual precipitation from 1920 to 2015 is recorded as 120 mm/yr while average seasonal cumulative precipitation from 1920 to 2015 is about 920 mm/yr. Crop production over East Africa is highly dependent on the long rainy season, which accounts for more than 70% of total annual precipitation. It is therefore, understandably that fluctuations in precipitation within this period is capable of altering and impacting food production across the region.

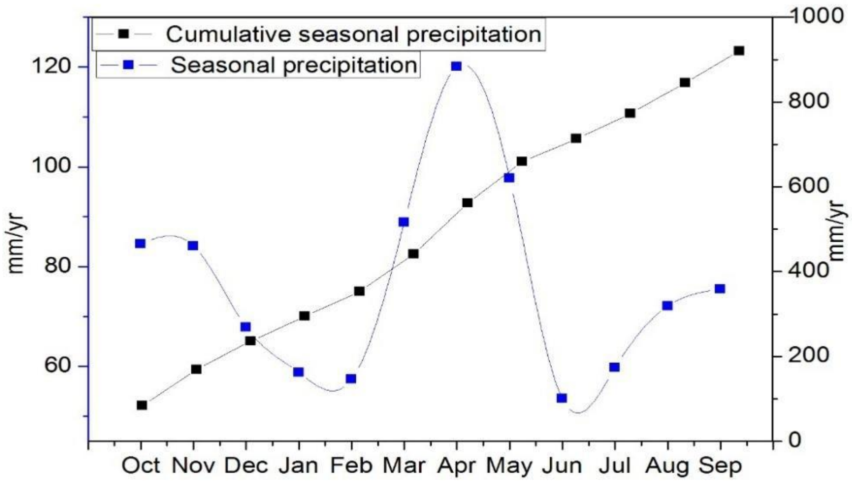

Fig. 2 Characteristics of precipitation over East Africa

Figure 3 shows precipitation anomalies from 1920 to 2015. Positive and negative anomalies represent wet and dry conditions, respectively, over East Africa. Based on the data used from 96 years (from 1920 to 2015) there are a total of 41 wet years and 46 drought years. The anomaly of the wet years and dry years were obtained when precipitation was above and below normal conditions, respectively, as seen in Fig. 3. The years 1961, 1967, 1997, 2007 and 2015 are the wettest while 1943, 1983, 1993, 1997 and 2003 are the driest. The annual precipitation, anomalies and the corresponding SPI's for wet and dry years are presented in Table 2. Results show that both wet and drought spells coincide with positive and negative anomalies over East Africa, respectively. This shows that the reason for the drought periods was as a result of unavailability of water in the soil. The magnitude of anomaly of the wet years was higher than that of the dry years and both wet and dry years were obtained when precipitation was above and below normal conditions, respectively. A detailed inspection of dry- and wet-year results also revealed that the chances of occurrence of wet years are greater in comparison to dry years. This information is important for the future planning and management of agricultural practices. This work has allowed us to identify years within the region that are prone to dry/wet conditions using available precipitation data records from 1920 to 2015.

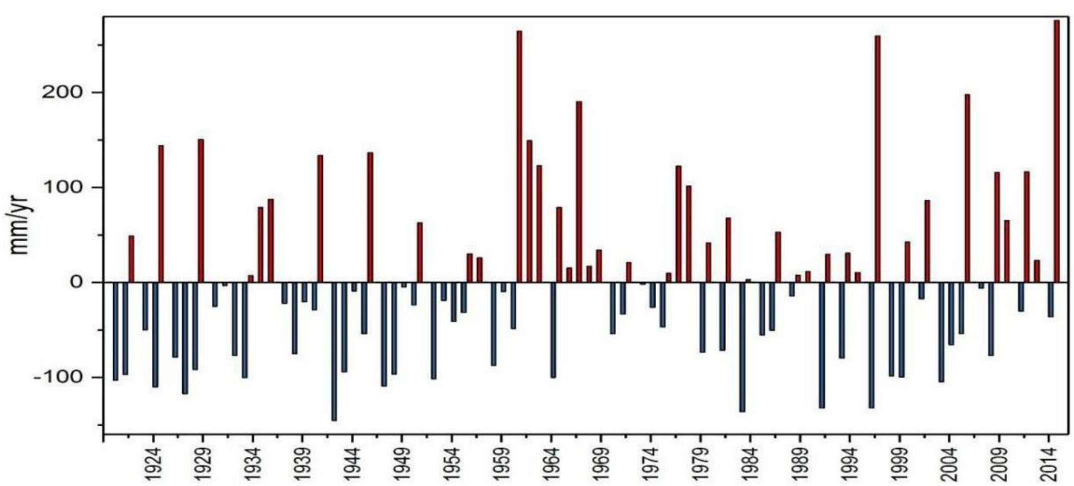

Fig. 3 Precipitation anomaly over East Africa

Table 2 Annual precipitation, anomaly and SPI-12

Condition	Yr	Annual precipitation (mm/yr)	Anomaly (mm/yr)	SPI
	1920-21	817.7	-102.8	-1.2
	1921-22	823.5	-96.9	-1.1
	1924-25	810.4	-110.0	-1.2
	1927-28	803.3	-117.2	-1.3
	1928-29	828.7	-91.7	-1.0
	1933-34	820.1	-100.3	-1.1
	1942-43	775.0	-145.4	-1.7*
Dry Spells	1943-44	826.4	-94.1	-1.0
	1947-48	811.3	-109.1	-1.2
	1948-49	823.7	-96.7	-1.1
	1952-53	818.9	-101.5	-1.1
	1964-65	820.4	-100.0	-1.1
	1983-84	784.2	-136.2	-1.6*
	1991-92	788.1	-132.3	-1.5*
	1996-97	788.2	-132.2	-1.5*
	1999-00	820.7	-99.7	-1.1
	2003-04	815.8	-104.7	-1.2

	Yr	Annual precipitation (mm/yr)	Anomaly (mm/yr)	SPI
	1925-26	1064.5	144.1	1.6
	1929-30	1071.0	150.6	1.6
	1941-42	1054.0	133.6	1.4
	1946-47	1056.9	136.5	1.5
	1961-62	1185.0	264.5	2.7**
	1962-63	1069.6	149.2	1.6
	1963-64	1043.2	122.8	1.3
	1967-68	1110.8	190.4	2.0**

Wet Spells	1977-78	1042.9	122.4	1.3
	1978-79	1021.9	101.5	1.1
	1997-98	1180.0	259.6	2.7**
	2002-03	1006.7	86.3	1.0
	2006-07	1118.2	197.8	2.1**
	2009-10	1036.0	115.6	1.3
	2012-13	1036.8	116.4	1.3
	2015-16	1196.4	275.9	2.8**

3.2. Spatial and temporal representation of spatial SPI over East Africa

Figure 4 shows the spatial representation of SPI for different hydrological years from 1920 to 2015 over East Africa. Results show that Figs. 4a, d and k recorded the highest precipitation while Fig. 4b, e and h recorded the least precipitation. It is critical to note that most of the regions that recorded the highest precipitation in some years also recorded the least in other years, hence establishing the fact that precipitation across most of the East African region is fluctuating and drought is not peculiar to one region.

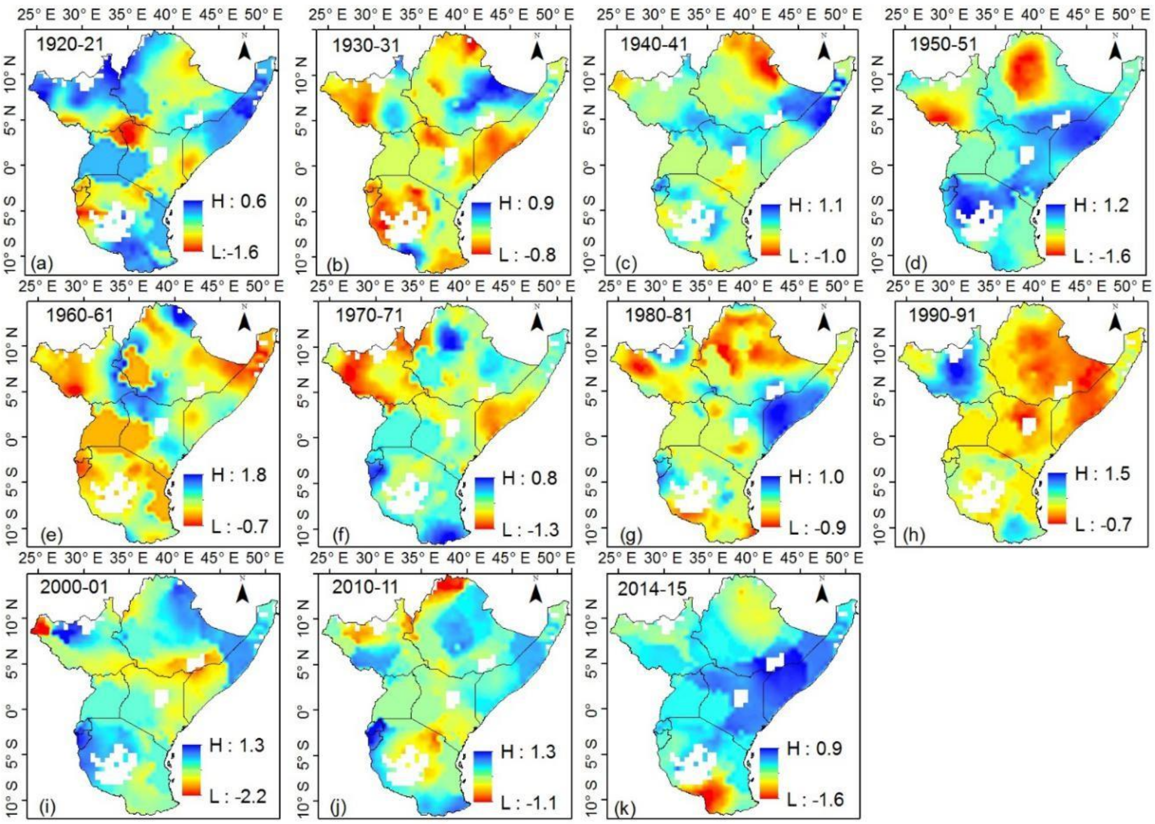

Fig. 4 Spatial representation of SPI for different hydrological years over East Africa

From Fig. 5, calculated SPI at different time scales of 3, 6 and 12 months indicated that for shorter time scales (i.e., 3 months, 6 months), there was a high temporal variability in dry and wet periods, whereas at longer time scales (12 months), frequency of dry and wet periods were considerably decreased.

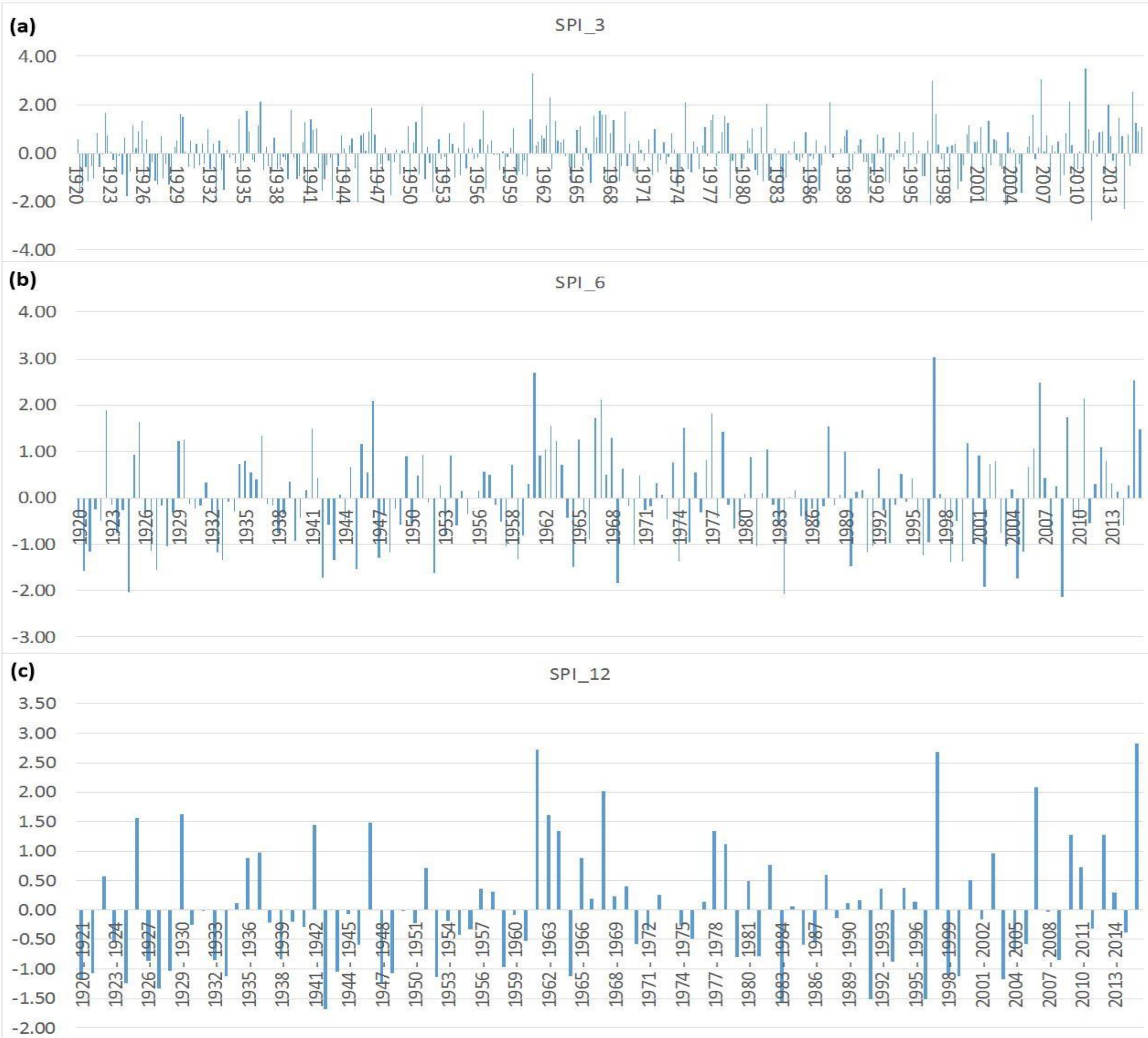

Fig. 5 (a) SPI-3 months (b) SPI-6 months (c) SPI-12 months

The drought magnitude, drought duration, and corresponding drought intensity were calculated over the study area (Table 3). And also, Fig. 6 shows drought magnitude over east Africa. Years with high drought magnitude ranged from 1922-22, 1926-29, 1942-46 and 1947-51 with values corresponding to 2.2, 3.2, 3.4 and 2.6, respectively while years with low drought magnitude ranged from 1930-31, 1988-89 and 2001-02 with values as 0.2, 0.12 and 0.15, respectively. Figure 7 shows drought duration in years over East Africa with the longest droughts occurring from 1929-29, 1937-41, 1942-46, 1947-51, 1952-56, and 1958-61 with values in years as 3, 4, 4, 4, 4, and 3 years, respectively, while the shortest droughts occurred in time period of 1 year and ranged from 1930-31, 1964-65, 1979-80, 1981-82, 1983-84, 1988-89, 1991-92, 1993-94, 1996-97 and 2001-02 (Also see Table 3). A comparison between Fig. 6 (drought magnitude) and Fig. 7 (drought duration) shows that not all the severest drought took longer and vice versa. Both drought magnitude and duration showed a negative slope of -0.071 and -0.086, respectively.

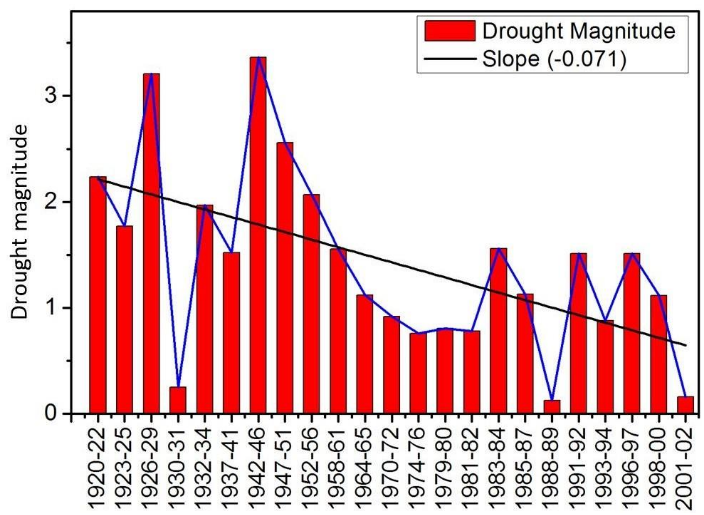

Fig. 6 Drought magnitude over East Africa

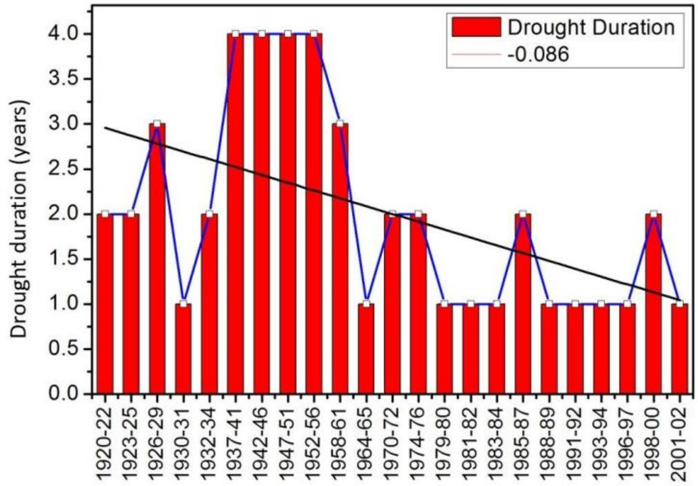

Fig. 7 Drought duration over East Africa

The drought magnitude was obtained as the cumulative SPI over the drought months taken as a positive value. The intensity (drought severity) was computed as the magnitude divided by drought duration. Among the droughts recorded, the drought of 1937-41, 1942-46, 1947-51, 1952-56 had the longest duration. Specifically, the results indicated that on one hand the frequency of drought events were high at shorter time scales but lasted for shorter durations at longer time intervals, and on the other hand droughts were less frequent but persisted for longer periods of time.

Table 3 Extraction of drought characteristics

Hydrological year	Magnitude	Duration	Intensity
1920-22	2.2333	2.000	1.1167
1923-25	1.7703	2.000	0.8852
1926-29	3.2102	3.000	1.0701
1930-31	0.2493	1.000	0.2493
1932-34	1.9668	2.000	0.9834
1937-41	1.5215	4.000	0.3804
1942-46	3.3653	4.000	0.8413
1947-51	2.5589	4.000	0.6397
1952-56	2.0666	4.000	0.5166

1958-61	1.5564	3.000	0.5188
1964-65	1.1191	1.000	1.1191
1970-72	0.9154	2.000	0.4577
1974-76	0.7563	2.000	0.3781
1979-80	0.8044	1.000	0.8044
1981-82	0.7803	1.000	0.7803
1983-84	1.5593	1.000	1.5593
1985-87	1.1279	2.000	0.5640
1988-89	0.1257	1.000	0.1257
1991-92	1.5109	1.000	1.5109
1993-94	0.8771	1.000	0.8771
1996-97	1.5102	1.000	1.5102
1998-00	1.1151	2.000	0.5576
2001-02	0.1588	1.000	0.1588

Figure 8 shows the spatial map of drought magnitude across the East African region for different hydrological years.

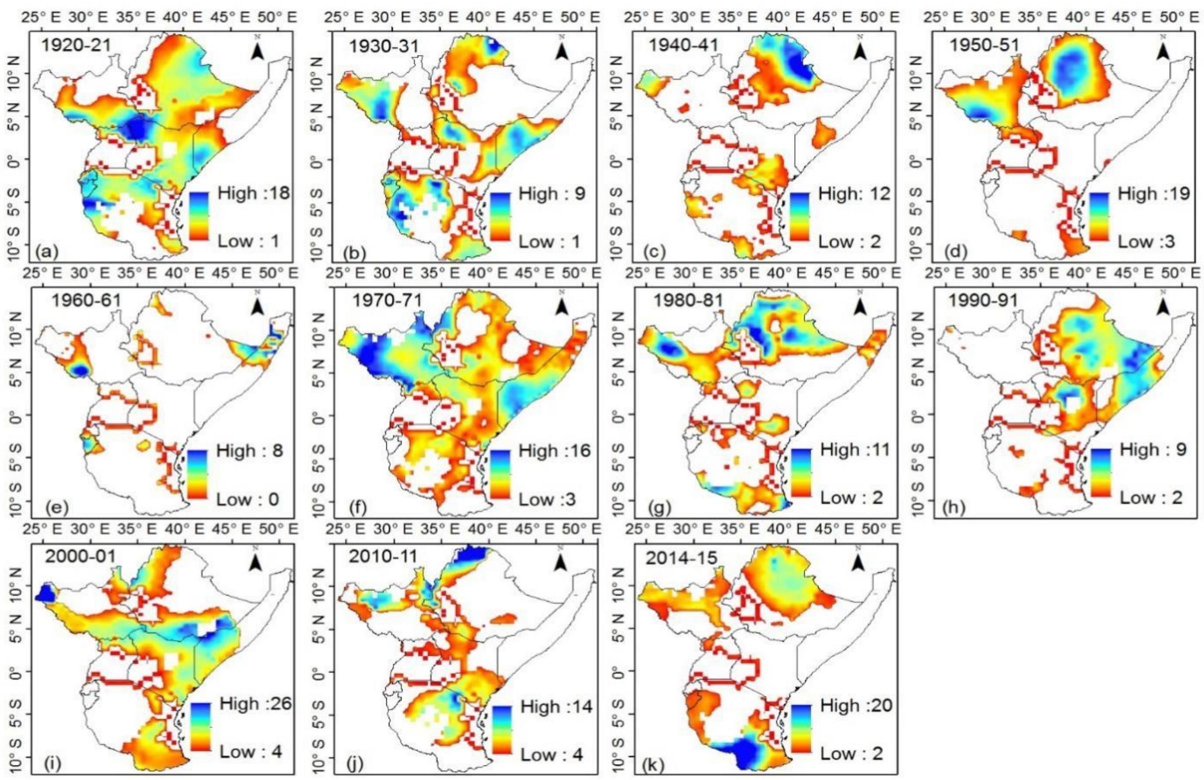

Fig. 8 Spatial drought magnitude over East Africa for different hydrological years

The results show that the drought magnitude is highest in 1920-21, 1950-51, 1970-71, 2000-01 and 2014-15 hydrological years. In 1920-21 hydrological year, regions that recorded high drought magnitude include South Sudan, Uganda, Kenya, Rwanda, Burundi and Eastern Tanzania. In 1950-51hydrological year, drought magnitude was highest over Ethiopia and South Sudan. In 1970-71 hydrological year, drought magnitude was highest over South Sudan, Ethiopia and Somalia. In 2000-01 hydrological year, drought magnitude was highest in South Sudan, Ethiopia, Somalia and Kenya. In 2014-15 hydrological year, drought magnitude was highest in Ethiopia and

Tanzania. This indicated that besides seasonal variability of spatial drought magnitude, there exist a strong variability of spatial drought magnitude across different decades.

3.3. Drought Risk Mapping and Joint Probability Distribution Function and Return years of Drought over East Africa

The spatial drought risk map was got from the spatial SPI map and represented in Fig. 9. It shows the spatial drought levels over East Africa across different decades, and changes across the region's land mass suggested to be as a result of changes in climate and land cover. There is high variability in drought across the decades over the region. These droughts could be categorized as ranging from moderate to extreme, with different durations and magnitudes. Nevertheless, the total duration, severity and magnitude of occurrence of the drought episodes varied from one location to another across the decades.

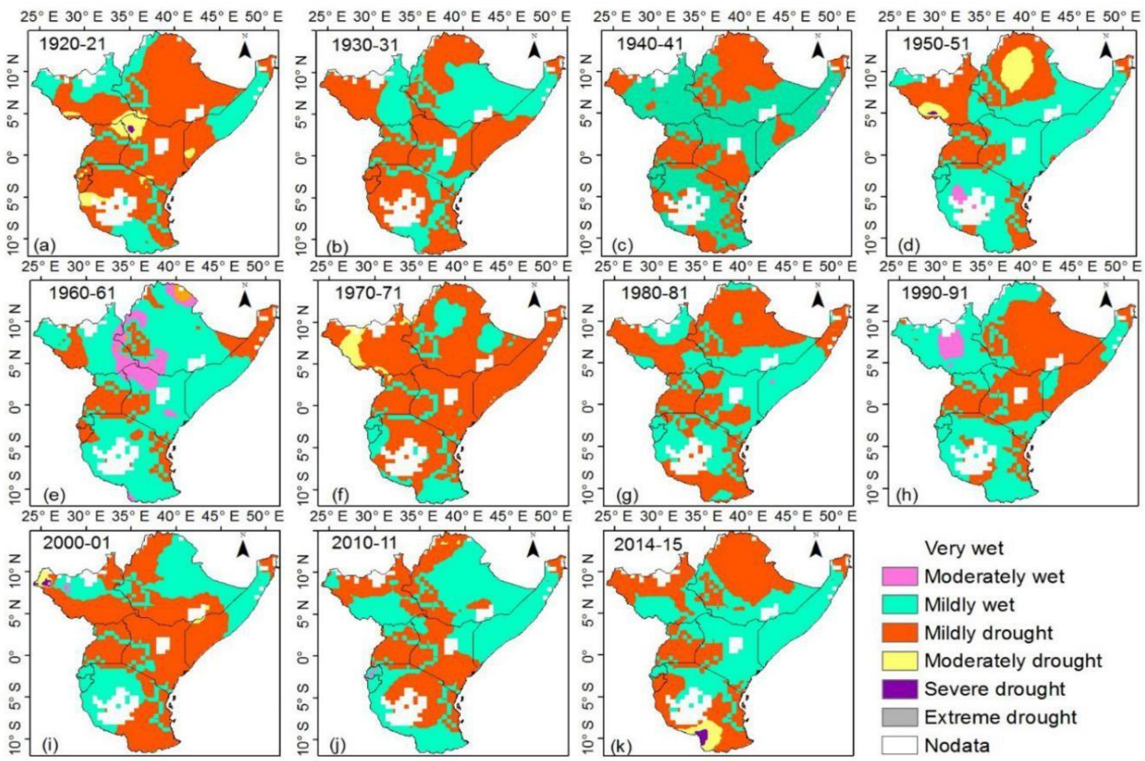

Fig. 9 The spatial drought risk map across East Africa

From Fig. 9, it appears as if drought repeats itself in some selected locations after a period of time but all droughts experienced in all locations and at all recorded periods appear to differ (see Figs. 9a to 9k). Drought may have similar magnitudes or duration but different levels of severity. For example, the droughts with magnitude (duration in years) of 1.5(4), 3.4(4), 2.6(4) and 2.0(4) lasted from 1937 to 1941, 1942 to 1946, 1947 to 1951 and 1952 to 1956, respectively (see Table 3). Since both drought severity and durations have different distributions, the Joint Probability Distribution Function (JPDF) given by equation (9) was used to obtain the probability Density function and the Joint return years were obtained using equation (10). The JPDF analysis is a useful multivariate tool needed for water resources management. Based on the drought characteristics, duration and magnitude using the 12-month SPI, the JPDF was estimated as shown in Figure 10.

From Fig.10, it shows that probability of drought occurrence is high when severity is low and such droughts occur at short time intervals. Also, it takes so many years for a severe drought to repeat itself at short time intervals.

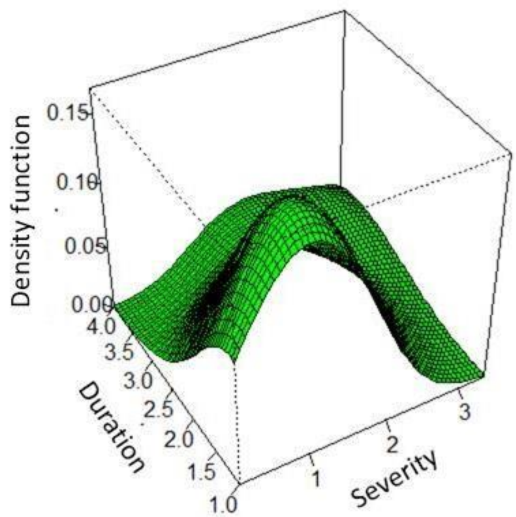

Fig.10 The JPDF for drought duration and severity (magnitude)

Once the JPDF for the bivariate return periods of drought was calculated, the drought severity duration frequency curve of East Africa was created (Fig.11). Fig.11 is a bivariate analysis of drought severity for East Africa region showing return periods and different levels of severity.

Drought severity itself is a function of the different drivers of drought over particular area. Drought severity characterizes drought magnitude of dry events. The JPDF drought-based curves were developed for selected recurrence severity levels of 5, 10, 20, 30, 40 and 50 years are plotted in Fig.11. It is observed that for any given duration, severe droughts have more return periods.

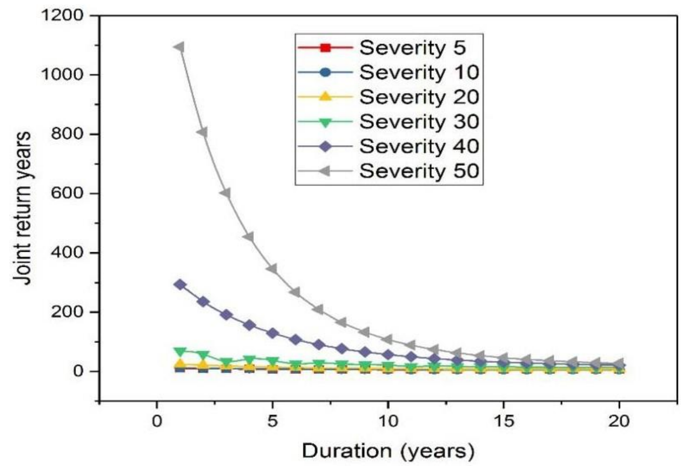

Fig. 11 Joint return years for severity (magnitude) corresponding to duration

Table 4 shows the drought occurrence over East African countries. The result shows that the drought mechanism is complex and the drivers highly depend on the local environmental conditions prevailing in a particular country. All drought episodes are associated with negative precipitation anomalies, low precipitation values closely matching the SPI values. The SPI values depicting drought levels (shown in Table 1) are applied to reveal the varying levels of drought experienced over specific countries in East Africa over the study period.

Table 4 Annual precipitation anomalies for various countries in East Africa from 1920-2015 with SPI-12. The value in parenthesis represents SPI

	Burundi	Rwanda	Ethiopia	Kenya	Somalia	Uganda	Tanzania	South Sudan
1920/21	-145 (-1.0)	-197 (-1.3)				-188(-1.4)		
1921/22	-383 (-3.0)							
1923/24	-174 (-1.2)	-231 (-1.5)						

1924/25			-93 (-1.0)	-150 (-1.2)		-190 (-1.4)	-165 (-1.3)	-84 (-1.0)
1926/27						-168 (-1.2)		-106 (-1.3)
1927/28	-259 (-1.9)	-225 (-1.5)		-125 (-1.0)		-155 (-1.1)		
1928/29	-216 (-1.6)	-158 (-1.0)		-128 (-1.0)		-144 (-1.0)	-191 (-1.5)	
1932/33			-96 (-1.1)	-163 (-1.4)				
1933/34	-285 (-2.1)	-291 (-2.0)				-163 (-1.2)		
1938/39			-95 (-1.0)		-72 (-1.0)	-191 (-1.4)		
1940/41			-102 (-1.1)					
1942/43	-203 (-1.5)	-237 (-1.6)	-146 (-1.7)	-129 (-1.0)		-215 (-1.6)		-123 (-1.5)
1943/44		-158 (-1.0)			-109 (-1.7)	-139 (-1.0)	-128 (-1.0)	
1945/46		-165 (-1.1)			-104 (-1.6)		-193 (-1.5)	
1947/48	-199 (-1.4)		-89 (-1.0)	-128 (-1.0)	-122 (-2.0)			
1948/49					-88 (-1.3)		-241 (-2.0)	
1950/51			-170 (-2.0)					-124 (-1.5)
1952/53			-100 (-1.1)			-177 (-1.3)	-222 (-1.8)	
1953/54					-72 (-1.0)			
1954/55					-106 (-1.6)			
1955/56			-130 (-1.5)		-117 (-1.8)			
1958/59	-193 (-1.4)				-68 (-1.0)		-162 (-1.3)	
1960/61	-211 (-1.5)	-148 (-0.9)					-164 (-1.3)	
1964/65			-121 (-1.4)	-140 (-1.2)	-80 (-1.2)	-213 (-1.6)	-148 (-1.1)	
1970/71					-86 (-1.3)			-99 (-1.2)
1971/72								-132 (-1.6)
1975/76				-183 (-1.6)				
1979/80			-113 (-1.3)	-149 (-1.2)	-77 (-1.1)	-189 (-1.4)		-110 (-1.3)

1981/82		-157 (-1.0)						-121 (-1.5)
1982/83								-125 (-1.5)
1983/84			-151 (-1.7)	-248 (-2.2)	-83 (-1.2)	-177 (-1.3)		-228 (-2.9)
1985/86			-114 (-1.3)					
1986/87			-105 (-1.2)					-218 (-2.8)
1989/90								-124 (-1.5)
1991/92	-144 (-1.0)	-151 (-1.0)	-155 (-1.8)	-147 (-1.2)	-156 (-2.7)	-154 (-1.1)		-97 (-1.2)
1993/94	-161 (-1.1)				-84 (-1.2)		-137 (-1.0)	
1996/97	-152 (-1.1)		-138 (-1.6)	-136 (-1.1)	-90 (-1.3)	-160 (-1.2)	-169 (-1.3)	-86 (-1.0)
1998/99		-166 (-1.1)	-104 (-1.2)	-171 (-1.4)	-87 (-1.3)			
1999/00	-158 (-1.1)	-209 (-1.4)		-161 (-1.3)			-254 (-2.1)	
2003/04		-250 (-1.7)	-141 (-1.6)	-161 (-1.3)		-177 (-1.3)		
2004/05				-160 (-1.3)		-178 (-1.3)		
2005/06		-175 (-1.1)					-139 (-1.1)	
2007/08						-142 (-1.0)		
2008/09								-150 (-1.9)
2010/11				-119 (-1.0)			-150 (-1.2)	
2011/12	-204 (-1.5)							

Note: 1920/21 represents a hydrological year starting in 1920 and ending in 1921.

The spatial and temporal variability in drought trends is observed in the study area and shown in Table 5 as the Negative and Positive SPI trends at multiple time scales across the East African countries. Of all the SPI models tested, only SPI-12 indicated significant trend values in Burundi, Rwanda and Uganda with Sen's slope (Kendal tau) values of 0.008 (0.143), 0.007 (0.144) and 0.008 (0.149) respectively. Basically, the SPI-12 shows the status of year-round water shortage caused by drought while SPI-6 and SPI-3 are appropriate indicators of the status of seasonal water shortage caused by drought (Tan et al., 2015).

Table 5 Mann-Kendall Trend and significance level of SPI-3, SPI-6 and SPI-12 over East African countries

Duration	Parameter	Burundi	Ethiopia	Kenya	Rwanda	South Sudan	Somalia	Tanzania	Uganda	Regional
SPI-3	Kendal τ	0.060	0.017	-0.004	0.089	-0.058	0.026	-0.028	0.062	0.036
	(Sign)	(0.086)	(0.635)	(0.914)	(0.011)	(0.097)	(0.450)	(0.419)	(0.074)	(0.307)
	Sen's slope	0.002	0.004	-0.0001	0.003	-0.005	0.002	-0.003	0.0002	-0.0001
	Trend	No	No	No	No	No	No	No	No	No
SPI-6	Kendal τ	0.073	0.008	0.006	0.087	-0.051	0.040	-0.057	0.087	0.037
	(Sign)	(0.140)	(0.879)	(0.908)	(0.079)	(0.305)	(0.421)	(0.247)	(0.079)	(0.457)
	Sen's slope	0.004	0.0001	-0.0003	0.004	-0.003	0.002	-0.003	0.005	0.002
	Trend	No	No	No	No	No	No	No	No	No
SPI-12	Kendal τ	0.143	-0.009	0.031	0.144	-0.071	0.072	-0.016	0.149	0.103
	(Sign)	(0.040)	(0.903)	(0.662)	(0.039)	(0.301)	(0.301)	(0.817)	(0.033)	(0.141)
	Sen's slope	0.008	-0.001	0.001	0.007	-0.004	0.004	-0.001	0.007	0.006
	Trend	Yes	No	No	Yes	No	No	No	Yes	No

Table 6 shows negative and positive precipitation trends at multiple time scales over East African countries. Out of eight countries, precipitation shows significant positive (insignificant positive) trends over 1(4) countries and significant (insignificant) negative trends over 1(2) countries from 1920 to 2015.

Table 6 Mann-Kendall Trend and significance level of precipitation over East African countries

Country	Kendal τ (sign)	Sen's slope	Trend
Burundi	0.023 (0.248)	0.021	No
Ethiopia	-0.001 (0.980)	-0.034	No
Kenya	0.005 (0.799)	0.006	No
Rwanda	0.034 (0.088)	0.092	No

South-Sudan	-0.044 (0.028)	-0.042	Yes
Somalia	0.048 (0.05)	0.007	Yes
Tanzania	-0.010 (0.603)	-0.010	No
Uganda	0.033 (0.101)	0.022	No
Regional	0.025 (0.216)	-0.005	No

3.4 Spatial trends in drought across East Africa

Figure 12 shows the spatial trend of SPI over East Africa. The approach involves running an Ordinary Linear Regression model to the SPI maps generated. Results show that about 28, 22 and 50 % of the SPI indicated spatial increase, no change and decrease in SPI trends respectively over the study area from 1920 to 2015. Increase (decrease) of SPI trends by our analysis means an increase (decrease) in moisture conditions corresponding to decrease (increase) in drought prevalence. Assessing the mean SPI drought characteristics over the region indicates that there were some notable variations in SPI, consistent with the distribution of precipitation. Areas with increase in SPI were located northeast, along the shores of the Indian Ocean and some few areas in the Central part of the study area. Areas with no trend changes in SPI were located in northwest, northeast, southeast parts of East Africa and close to the shores of the ocean. Also, areas with decreasing SPI trend pixels were located around in the Northwest, Northeast, and Southwest and along the shores of the study area. The 96-year precipitation records in areas with spatial increase in SPI trend were 11.3, 136.5, 77.3 and 26.5 mm for minimum, maximum, mean and standard deviation values respectively while the precipitation records in areas with spatial decrease in SPI were 539, 138.3, 56.1 and 29.7 for minimum, maximum, mean and standard deviation values respectively. For areas with no spatial trend changes in SPI were 7.2, 161.6, 93.2 and 31.9 for minimum, maximum, mean and standard deviation values, respectively. Areas with improvement in drought indicated the low precipitation standard deviation. Our result confirms that areas with no SPI changes in drought were wetter from 1920 to 2015.

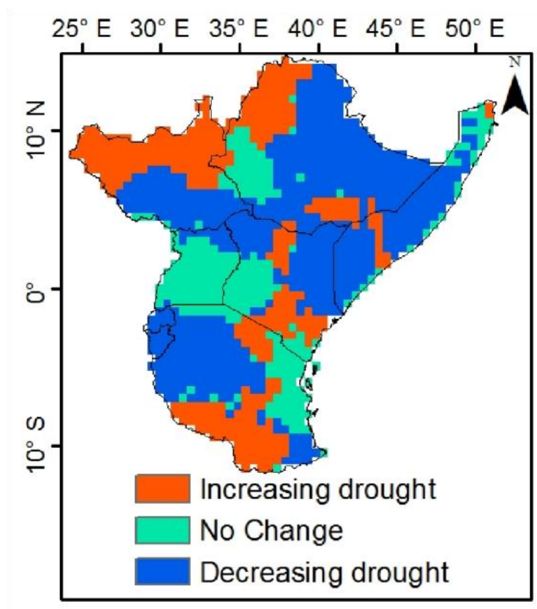

Fig.12 Spatial trends in SPI over East Africa

Figure 13a shows the spatial slope of SPI versus latitudes (degrees). Results indicate that high of SPI slope are clustered at higher latitudes from latitude 0 to 12^{o} while low trend values are clustered between latitude -2 and 2^{o} south of the study region which is an indication that drought is prevalent in the northern section than southern section of the study area.

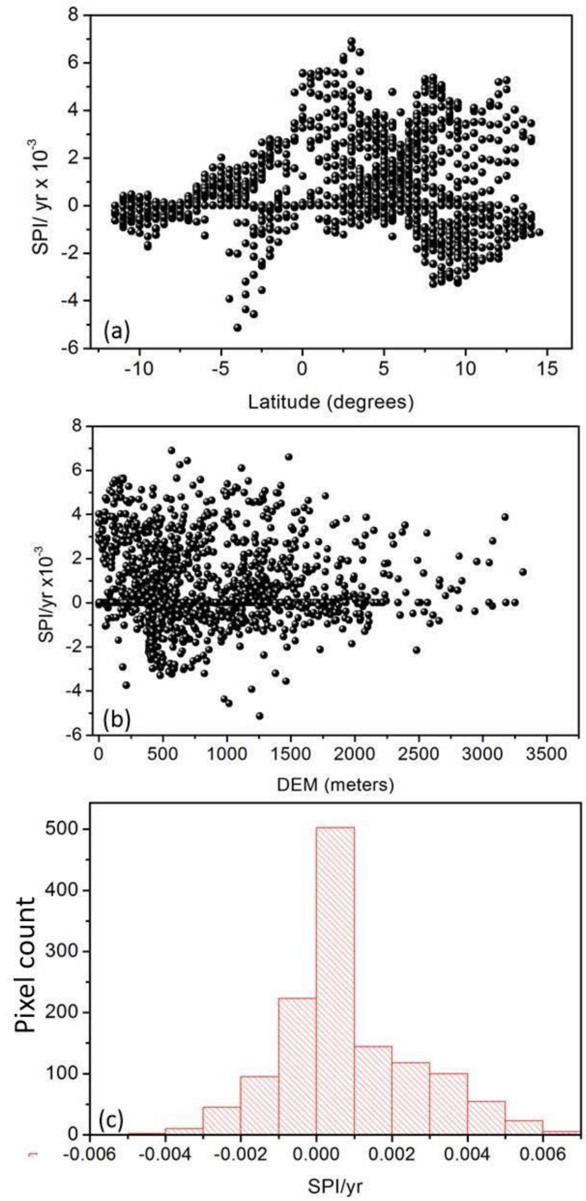

Fig.13 (a) SPI slope versus latitude (b) SPI slope versus DEM and (c) histogram of pixel count

Figure 13b shows SPI slope versus DEM where both high and low slope values of SPI are clustered at lower latitudes between 0 to 1500 m, and at the foot hills of mountains. The histogram of the SPI trends is shown in Figure 13c. It can be observed that most of the SPI trends are clustered around the 0.0 mark, which shows that the density curve of the pixels is symmetrical and centered about its mean. The SPI trends indicate high positive (negative) pixels above (below) the zero trend mark, implying that drought prevails in both low and high elevation areas up to 2000 m.

3.5 ENSO-drought relationship

Drought is considered as one of the most complex and deleterious natural, with severe impacts on natural ecosystems, water resources and food security (Tan et al., 2015). In this study, we selected the El Niño, neutral, and La Niña years based on data from sea surface temperature (SST) anomalies of the tropical Indian Ocean in the region + 0.5 °C and – 0.5 °C also known as the Niño 3.4 region. The gridded Extended Reconstructed Sea Surface Temperature version 4 (ERSSTv4) temperature data was used to study the ENSO events. We considered El Niño (La Niña) years as years with average SST anomalies above (below) temperature values of +0.5 °C (−0.5 °C) from October to March. The October to March period typically coincides with peak ENSO Conditions Neutral years if the SST values are within - 0.5 °C < SST < 0.5 °C as shown in Fig. 14.

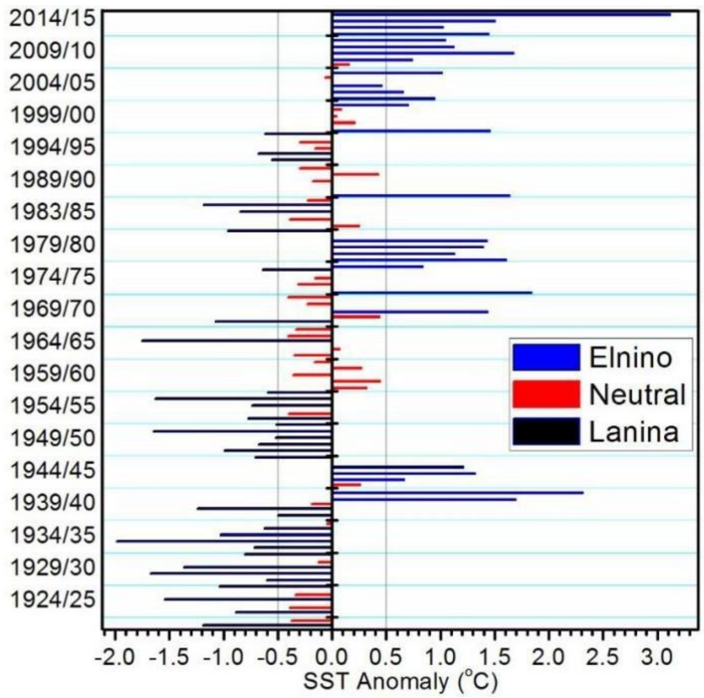

Fig. 14 Extended reconstructed sea surface temperature showing El Niño, neutral and La Niña years.

The SPI values in neutral, El Niño, and La Niña years were studied over East Africa from 1920 to 2015. The mean drought characteristics, magnitude, duration and even the dispersion, of drought magnitude in SPI-3, SPI-6 and SPI-12 are very similar in El Niño and La Niña events while the neutral years presented high dispersion in both drought magnitude and duration (Fig.15).

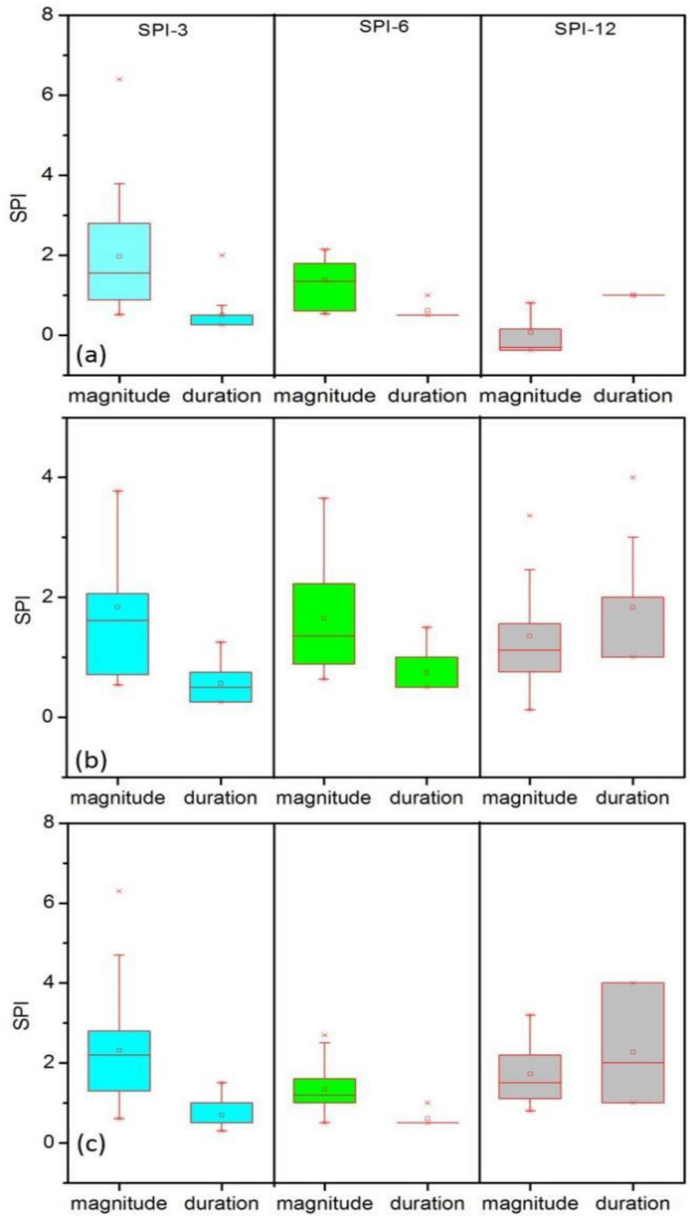

Fig. 15 Boxplots of mean magnitude and duration for (a) El Niño (b) neutral and (c) La Niña years

Results shown on Fig. 15a indicate that the mean drought duration during El Niño years were less than 1.5 years while the mean drought duration during neutral (La Niña) years was 3 (4) years (Figs. 15b and c).

In this study, there is no direct link between ENSO and drought over the East African region. But the association of drought in most El Niño and La Niña years suggests that the impact of

ENSO cannot be ruled out. Our results have supported reports that present teleconnections between drought and ENSO. Previous reports have shown that ENSO events normally peak during October to March periods which coincides with the short (SON) and long (MAM) rainy seasons of East Africa. This period coincides with the SON and MAM seasons and increased precipitation in East Africa. Considering the major drought episodes over the East Africa, our analysis has only agreed with the major droughts of 2011/12. Based on our results, 2011/12 was captured as an El Niño year with drought magnitudes captured by SPI-3 and SPI-6 as 2.8 and 0.5 respectively with drought duration of 3 and 6 months, respectively. The drought episode of 2011/12 affected countries like Somalia, Uganda, Kenya, Ethiopia, South-Sudan and other nearby countries.

3.6. Discussion

Generally, the actual precipitation expressed as a percentage deviation from normal (or long-term average) is the most commonly used drought indicator, although it has limited use/reliability for spatial comparison due to its dependence on the mean (Kumar et al., 2009). According to Solanki and Parekk (2014), the SPI represents a departure from the mean and is thus, expressed in standard deviation units as a normalized index in time and space. The departure from the mean is a probability indication of the severity of the wetness or drought that can be used for risk assessment. The application of data from 1920 in this study is considered most desirable as long records provide more reliable statistics for SPI, given that it is a statistical approach. As a result, SPI has gained importance in recent years as a potential drought indicator permitting comparisons across different precipitation zones (Kumar et al., 2009; Solanki and Parekk, 2014).

This study analyzed SPI values between 1920 and 2016 with actual precipitation and precipitation deviation from normal in East Africa, a generally low precipitation and drought prone region. The objective is to establish whether or not SPI can be used as a suitable indicator (when compared to conventionally adopted precipitation deviation-based approach for drought intensity assessment) over an extended region such as East Africa.

The results of the analysis show that very low or very high precipitation corresponded to very low or very high SPI values. Thus, SPI values adequately estimated the dryness or wetness when the precipitation is very low or very high, respectively. Table 2 shows that all periods that experienced dry spells (or drought) recorded low/negative anomaly and SPI values with the periods 1942-1943 recording the driest (-1.7) followed by 1983-1984 (-1.6). Similarly, the periods of wet spells reveal positive anomaly and SPI values with the wettest period being 2014-2015. The outcome of this study is in line with the SPI classes proposed by McKee et al. (1993). However, there is a marked variation between drought characteristics of magnitude, duration and intensity when viewed against temporal scales. In essence, no time scale recorded the highest in all 3 drought characteristics throughout the 95-year period of analysis (Table 3). This is similar to the observation of SPI at different time scales of 3, 6 and 12 months which reveal that for shorter time scales, there was a high temporal variability in dry and wet periods, whereas at longer time scales (12 months), frequency of dry and wet periods were considerably decreased (Fig. 5).

The results of this study indicate that drought characteristics analysis (magnitude, duration and intensity) using SPI can be adequately applied for drought intensity assessment particularly in regions such as East Africa where low precipitation and vulnerability to droughts is prevalent. The precipitation anomalies (Table 4), Mann-Kendall Trend and significance level of SPI-3, SPI-6 and SPI-12 (Table 5) and Mann-Kendall Trend and significance level of precipitation (Table 6) reveal varying results both temporally and spatially across the eight countries comprising the East African region covered in this study. For instance, the same drought level (SPI) may be prevalent in a country but the precipitation anomaly values may differ (Table 4). The drought of 1942-43 was worst hit in countries like Burundi, Rwanda, Ethiopia, Uganda and South-Sudan.

From 1983-84, Ethiopia, Kenya, Somalia, Uganda and South-Sudan experienced the worst drought episodes. Also, from 1991-92, Ethiopia, Kenya, and Somalia experienced worst drought spells, while in 1996-97, the highest effect was observed in Ethiopia. Table 5 reveals that out of eight countries, SPI-12 detects significant positive (insignificant positive) trend over 3(2) countries and insignificant negative trends over 3 countries. SPI-6 detects insignificant positive trend over 6 countries and insignificant negative trend over 2 countries. SPI-3 detects insignificant positive trends over 5 countries while insignificant negative trends in 3 stations. At regional (continental scale), there was no significant trend in SPI-3, SPI-6 or SPI-12. The results in Table 6 show that most countries experience oscillations between wet and dry conditions while few countries are getting wetter with few others getting more arid. At regional (continental scale), there was no significant trend in precipitation. There was no significant change in precipitation in annual rainy seasons during the study period. As no annual trend was observed in the precipitation amount, we applied SPI to study precipitation address potential changes in precipitation extremes.

There is expected to be some time lag due to the unique vegetation types which, according to Abbas et al. (2014), should have different capacity of water storage. The humid area covering most of Uganda as shown on Fig. 1 (with predominantly tall and dense forests) are expected to have a longest time lag because, according to Allen (2008), forests possess the best capacity of water retention with deeper roots to tap groundwater. Conversely, arid and semi-arid areas such as Kenya, Somalia and Ethiopia are covered mostly by grasses and should have shorter time lag due to the lower capacity of water retention for grasses. South-Sudan and a significant area of Tanzania are sub-humid areas largely covered by crops. Generally, the water storage capacity of crops is likely similar to or even lower than that of grasses, and Grünzweig et al. (2015) posits that artificial irrigation could alter the time lag for regions engaged in irrigation agriculture. It is therefore, expected that semi-arid areas should have a time lag similar to or longer than arid areas (Cong et al., 2017). This pattern is largely similar to the outcome of the study as shown on Tables 4, 5 and 6, and Figs 4, 8 and 9.

4. Conclusions

In this study, the SPI approach applied to this study adequately explained the drought conditions across the East African region between 1920 and 2015. The drought characteristics of magnitude, duration and intensity collectively explained the severity levels of drought within the study area. It is expected that the outcome of this study could be applied elsewhere in sub-Saharan Africa where precipitation is limited and likelihood of drought is high.

The result from the 96 years (from 1920 to 2015) data records shows that there are a total of 41 wet years and 46 drought years. The anomaly of the wet years and dry years were obtained when precipitation was above and below normal conditions respectively. The years 1961, 1967, 1997, 2007 and 2015, were adjudged the wettest while 1943, 1983, 1993, 1997 and 2003 were adjudged the driest. Both the positive and negative peak of SPI coincided with the positive and negative anomaly peaks, respectively. The computed SPI at different time scales of 3, 6 and 12 months indicated that for shorter time scales, there was high temporal variability in dry and wet periods, whereas at longer time scales (12 months), frequency of dry and wet periods were considerably decreased.

Years with high drought magnitude ranged from 1920-22, 1926-29, 1942-46 and 1947-51 with SPI values corresponding to 2.2, 3.2, 3.4 and 2.6, respectively while years with low drought magnitude ranged from 1930-31, 1988-89 and 2001-02 with values as 0.2, 0.12 and 0.15, respectively. The longest droughts occurred from 1929-29, 1937-41, 1942-46, 1947-51, 1952-56, and 1958-61 with values in years as 3, 4, 4, 4, 4, and 3 years, respectively, while the shortest droughts occurred in time period of 1 year and ranged from 1930-31, 1964-65, 1979-80, 1981-82, 1983-84, 1988-89, 1991-92, 1993-94, 1996-97 and 2001-02.

Our study also indicated that high values of SPI slope are clustered at higher latitudes from 0 to 12^o while low trend values are clustered between -2 and 2^o south of the study region which is an indication that drought is prevalence in the northern section than southern section of the study area.

Both high and low slope values of SPI are clustered at lower latitudes between 0 to 1500 meters, and at the foot hills of mountains. The SPI trends showed high positive (negative) pixels above (below) the zero-trend mark, indicating that drought prevails in both low and high elevation areas up to 2000 m.

In terms of ENSO impacts on drought over the region, the mean characteristics, magnitude, duration and even the dispersion, of drought magnitude in SPI-3, SPI-6 and SPI-12 are very similar in El Niño and La Niña years while the neutral years presented high dispersion in both drought magnitude and duration. The mean drought duration during El Niño years were less than 1.5 years while the mean drought duration during neutral (La Niña) years was 3 (4) years which suggest that there is no direct link between ENSO and drought over the East African region. But the association of drought in most El Niño and La Niña years suggests that the impact of ENSO cannot be ruled out since peak ENSO events occur during October to March periods which coincides with the short (SON) and long (MAM) rainy seasons of East Africa.

Furthermore, the outcome of this study indicates that SPI can be reliably suitable and most applicable in drought studies within the study area as it provides for analysis in multi-temporal levels such as monthly, single seasonal, multi-seasonal, and annual droughts, thereby allowing for a spatio-temporal scale of analysis that creates the room for SPI to provide accurate meteorological and agricultural drought analysis. To this extent, the study provides policy makers the necessary information that is critical to local adaptation, increased resilience and mitigation measures in the face of a vulnerable eco-climatic system triggered by a continuously changing climate within East Africa as well as other parts of sub-Saharan Africa.

Our study is particularly relevant in its ability to depict continuous and synoptic drought conditions all over East Africa, providing vital information to farmers and policy makers, using very cost-effective method. This is particularly the case in view of the assertion by Karavitis et al. (2011) that “effective (and reliable) information and early warning systems based on indicators such as the SPI are the foundation for overall effective drought adaptation (and resilience) plans”. Finally, the adoption of SPI for this study demonstrates the fact that it is a robust concept, unambiguous in calculation and understanding, temporally flexible, spatially meaningful, and widely applicable, a basis for which it is considered a powerful tool for drought studies as clearly amplified by Cheval (2015).

Acknowledgements

This work was jointly supported by the CAS Strategic Priority Research Program (No. XDA19030402), the National Key Research and Development Program of China (no. 2016YFD0300101), and “Taishan Scholar” Project of Shandong Province (No. TXXD 201712). The authors would like to show great appreciations to the anonymous reviewers and the editor for their valuable comments and suggestions.

References

Abbas, S., Nichol, J.E., Qamer, F.M., Xu, J. (2014). Characterization of drought development through remote sensing: A case study in central Yunnan, China. Remote Sens. 6(6): 4998–5018.

Abbink, J., K. Askew, D.F. Dori, E. Fratkin, E.C. Gabbert, J. Galaty, S. LaTosky, J. Lydall, et al., (2014). Lands of the Future: transforming pastoral lands and livelihoods in eastern Africa. Working Paper No. 154, Max Planck Institute for Social Anthropology.

Allen, C.D. (2008). Mechanisms of plant survival and mortality during drought: why do some plants survive while others succumb to drought? New Phytol. 178 (4), 719.

American Meteorological Society (1997). Meteorological drought-policy statement. Bull Am Meteorol Soc 78:847–849

Bates, B.C., Kundzewicz, Z.W., Wu, S.and Palutikof, J.P. (eds.). (2008). Climate Change and Water. Technical Paper of the Intergovernmental Panel on Climate Change, IPCC Secretariat, Geneva. Available from https://www.ipcc.ch/pdf/technical-papers/climate-change-water-en.pdf - 28/doc13.pdf (accessed: June, 2018).

Cong, D., S. Zhao, C. Chen and Z. Duan (2017). Characterization of droughts during 2001–2014 based on remote sensing: A case study of Northeast China. Ecological Informatics 39: 56–67

Dai, A., Lamb, P., Trenberth, K.E., Hulme, M., Jones, P.D. and Xie, P. (2004) The Recent Sahara Drought is Real. International Journal of Climatology 24: 1323-1331

Eze, J.N. (2018) Drought occurrences and its implications on the households in Yobe state, Nigeria. Geoenvironmental Disasters 5:18, 1-10

Funk, C., Dettinger, M. D., Michaelsen, J. C., Verdin, J. P., Brown, M. E., Barlow, M., & Hoell, A. (2008). Warming of the Indian Ocean threatens eastern and southern African food security but could be mitigated by agricultural development. Proceedings of the National Academy of Sciences, 105(32), 11081-11086.

Funk, C., Hoell, A., Shukla, S., Bladé, I., Liebmann, B., Roberts, J. B., Robertson, F. R., and Husak, G. (2014) Predicting East African spring droughts using Pacific and Indian Ocean sea surface temperature indices, Hydrol. Earth Syst. Sci., 18, 4965–4978, https://doi.org/10.5194/hess-18-4965-2014.

Funk, C., Husak, G., Michaelsen, J., Shukla, S., Hoell, A., Lyon, B., et al. (2013). Attribution of 2012 and 2003-12 rainfall deficits in eastern Kenya and southern Somalia. In Explaining extreme events of 2012 from a climate perspective. Bulletin of the American Meteorological Society. 94, S45-S48.

Funk, C., Peterson, P., Landsfeld, M., Pedreros, D., Verdin, J., Shukla, S., Husak, G., Rowland, J., Harrison, L., Hoell, A., and Michaelsen, J. (2015) The climate hazards infrared precipitation with stations-a new environmental record for monitoring extremes, Sci. Data, 2, 150066, https://doi.org/10.1038/sdata.2015.66

Ghulam A, Qin Q, Zhan Z (2007a) Designing of the perpendicular drought index. Environ Geol 52(6):1045–1052

Ghulam A, Qin Q, Teyip T, Li Z-L (2007b) Modified perpendicular drought index (MPDI): a real-m time drought monitoring method. ISPRS J Photogramm Remote Sens 62:150–164

Gibbs W., Maher J. (1967) Rainfall deciles as drought indicators. Australian Bureau of Meteorology Bulletin, Melbourne: 48

Grünzweig, J.M., Valentine, D.W., Chapin III, F.S. (2015). Successional changes in carbon stocks after logging and deforestation for agriculture in Interior Alaska: implications for boreal climate feedbacks. Ecosystems 18 (1), 132–145

Hao, C., Zhang, J., Yao, F. (2015). Combination of multi-sensor remote sensing data for drought monitoring over Southwest China. J. Appl. Earth Obs. Geoinf. Int. https://doi.org/10.1016/j.jag.2014.09.011.

Harvest Choice (2015). "AEZ tropical (5-class, 2009)." International Food Policy Research Institute, Washington, DC., and University of Minnesota, St. Paul, MN. Available online at http://harvestchoice.org/data/aez5_clas

Haroon, M.A., Zhang, J. and Yao, F. (2016). Drought monitoring and performance evaluation of MODIS-based drought severity index (DSI) over Pakistan. Natural Hazards 84(2): 1349-1366

Huete, A. (1988) A soil-adjusted vegetation index (SAVI). Remote Sens Environ 25:295–309

Igbawua, T., Zhang, J., Yao, F., Zhang, D. (2018). Assessment of moisture budget over West Africa using MERRA-2’s aerological model and satellite data. Climate Dynamics https://doi.org/10.1007/s00382-018-4126-2

Kalisa, W., Igbawua, T., Henchiri, M., Ali, S., Zhang, S., Bai, Y., Zhang, T. (2019) Assessment of climate impact on vegetation dynamics over East Africa from 1982 to 2015. Scientific Reports, | 9:16865 | https://doi.org/10.1038/s41598-019-53150-0

Karavitis, C.A., S. Alexandris, D.E. Tsesmelis and G. Athanasopoulos (2011). Application of the Standardized Precipitation Index (SPI) in Greece. Water, 3: 787-805; doi:10.3390/w3030787

Kim, T., Yoo, C., Valdes, J.B. (2003) Non parametric Approach for estimating effects of ENSO on return periods of Drought, Water Engineering, 7(5), 629-636.

Kogan, F.N. (1995) Application of vegetation index and brightness temperature for drought detection. Adv Space Res 15:91–100

Kogan, F.N. (2001) Operational space technology for global vegetation assessment. Bull Am Meteorol Soc 82:1949–1964

Kogan, F.N., Gitelson, A., Zakarin, E., Spivak, L., Lebed L (2003) AVHRR-based spectral vegetation index for quantitative assessment of vegetation state and productivity: calibration and validation. Photogramm Eng Remote Sens 69:899–906

Kumar, M.N., C.S. Murthy, M.V.R. Sesha-Saib and P.S. Roy (2009). On the use of Standardized Precipitation Index (SPI) for drought intensity assessment Wiley Inter Science Meteorol. Appl. 16: 381–389

Lambin, E., Ehrlich, D. (1995) Combining vegetation indices and surface temperature for land-cover mapping at broad spatial scales. Int J Remote Sens 16:573–579

Lei, T., Pang, Z., Wang, X., Li, L., Fu, J., Kan, G., et al. (2016). Drought and carbon cycling of grassland ecosystems under global change: a review. Water 8(10), 460.

Liu, H.Q., Huete, A. (1995) A feedback based modification of the NDVI to minimize canopy background and atmospheric noise. IEEE Trans Geosci Remote Sens 33:457–465

Liu, Q., Zhang, S., Zhang, H., Bai, Y., Zhang, J. (2019) Monitoring drought using composite drought indices based on remote sensing. Science of the Total Environment 711 (2020) 134585.

Love, R. (2009) Economic Drivers of Conflict and Cooperation in the Horn of Africa, Chatham House Briefing Paper, December, available at: www.chathamhouse.org/ publications/papers /view/109208 (last access: 18 April 2012).

Masih, I., Maskey, S., Mussá, F.E.F. a0nd Trambauer, P. (2014) A review of droughts on the African continent: a geospatial and long-term perspective, Hydrol. Earth Syst. Sci., 18, 3635–3649, https://doi.org/10.5194/hess-18-3635-2014

McKee, T.B., Doesken, N.J. and Kleist, J. (1993) The relationship of drought frequency and duration to time scales. *In*: Eighth conference on applied climatology. American Meteorology Society, Anaheim, CA, 179–184

McQuigg, J. (1954). A simple index of drought conditions. Weather Wise 7:64–67

Morton, J. and Kerven, C. (2013). Livelihoods and basic service support in the drylands of the Horn of Africa. Brief prepared by a Technical Consortium hosted by CGIAR in partnership with the FAO Investment Centre. Technical Consortium Brief 3. Nairobi: International Livestock Research Institute.

Mu, Q., Zhao, M., Kimball, J.S., McDowell, N.G., Running, S.W. (2013). A remotely sensed global terrestrial drought severity index. Bull Am Meteorol Soc 94:83–98

Munger, T.T. (1916). Graphic method of representing and comparing drought intensities. Monthly Weather Rev 44:642–643

Niemeyer, S. (2008). New drought indices. Options Mditerranennes Sri A Sminaires Mditerranens 80:267–274

O'Connor, T.G. (1995). Transformation of a savanna grassland by drought and grazing. African Journal of Range and Forage Science. 12 (2): 53–60.

Palmer, W.C. (1968). Keeping track of crop moisture conditions, nationwide: the new crop moisture index. Weather Wise 21: 156–161

Pramudya, Y. and T. Onishi (2018). Assessment of the Standardized Precipitation Index (SPI) in Tegal City, Central Java, Indonesia. IOP Conf. Series: Earth and Environmental Science 129: 1-9

Sandholt, I., Rasmussen, K., Andersen, J. (2002). A simple interpretation of the surface temperature/vegetation index space for assessment of surface moisture status. Remote Sens Environ 79:213–224

Schubert, S.D., Stewart, R.E.,Wang, H., Barlow,M., Berbery, E.H., Cai,W., et al., (2016). Global meteorological drought: a synthesis of current understanding with a focus on SST drivers of precipitation deficits. J. Clim. 29 (11), 3989–4019.

Solanki, J.K. and F, Parekh (2014) Drought Assessment Using Standardized Precipitation Index International Journal of Science and Research, 3(7): 1073-1076

Svoboda, M.D., LeComte, D., Hayes, M.J. (2002). The drought monitor. Bull Am Meteorol Soc 93:1181–1190

Tan, C., Yang, J., Li, M., 2015 Temporal-Spatial Variation of Drought Indicated by SPI and SPEI in Ningxia Hui Autonomous Region, China, Atmosphere, 6, 1399-1421; doi:10.3390/atmos6101399

Tarhule, A., Woo, M.-K. (1997). Towards an interpretation of historical droughts in northern Nigeria. Climatic Change 37: 601–616

Um, M., Y. Kim, D. Park, and J. Kim. (2017). Effects of different reference periods on drought index estimations from 1901 to 2014. Hydrology and Earth System Sciences 21: 4989–5007

von Grebmer, K., Bernstein, J., Nabarro, D., Prasai, N., Amin, S., Yohannes, Y., Sonntag, A., Patterson, F., Towey, O., Thompson, J. (2016). Global Hunger Index: Getting to Zero Hunger. Welthungerhilfe, International Food Policy Research Institute, and Concern Worldwide, Bonn, Washington, DC, and Dublin

Waggoner, M.L. and O'Connell, T.J. (1956). Antecedent precipitation index. Weekly Weather Crop Bull XLIII: 6–7

Weghorst, K. (1996) The reclamation drought index: guidelines and practical applications. Bureau of Reclamation, Denver

Yang, H. and Huntingford, C. (2018). Drought likelihood for East Africa. Nat. Hazards Earth Syst. Sci., 18: 491–497

Yao, N., Y. Li., T. Lei. and L. Peng. (2018). Drought evolution, severity and trends in mainland China over 1961–2013. Science of the Total Environment 616–617: 73–89

Yao, Y., Liang, S., Qin, Q., Wang, K. (2010). Monitoring drought over the conterminous United States using MODIS and NCEP Reanalysis-2 data. J. Appl. Meteorol. Climatol. 49: 1665–1680

Conflict of Interest

We declare that we do not have any commercial or associative interest that represents a conflict of interest in connection with the work submitted.

Correspond author: Jiahua

Zhang email: zhangjh@radi.ac.cn

Tel: 0086-13683576879